microbial biotechnology

Open Access

The potential of bacteriophages to control *Xanthomonas campestris* pv. *campestris* at different stages of disease development

Dominique Holtappels,[1] Kiandro J. Fortuna,[1] Lauren Moons,[1] Nand Broeckaert,[1] Léon E. Bäcker,[2] Sofie Venneman,[3] Sofie Rombouts,[1,4] Louis Lippens,[5] Steve Baeyen,[4] Sabien Pollet,[6] Jean-Paul Noben,[7] Frank Oechslin,[8] Marta Vallino,[9] Abram Aertsen,[2] Martine Maes,[10] Johan Van Vaerenbergh,[4] Rob Lavigne[1,] and Jeroen Wagemans[1,*]**

[1]*Laboratory of Gene Technology, KU Leuven, Leuven, Belgium.*
[2]*Laboratory of Food Microbiology, KU Leuven, Leuven, Belgium.*
[3]*Proefstation voor de groenteteelt, Sint-Katelijne-Waver, Belgium.*
[4]*Flanders Research Institute for Agriculture, Fisheries and Food, Ghent, Belgium.*
[5]*Provinciaal Proefcentrum voor de Groenteteelt Oost-Vlaanderen, Kruishoutem, Belgium.*
[6]*Inagro, Beitem, Belgium.*
[7]*Biomedical Research Institute and Transnational University Limburg, Hasselt University, Hasselt, Belgium.*
[8]*Department of Fundamental Microbiology, University of Lausanne, Lausanne, Switzerland.*
[9]*Institute for Sustainable Plant Protection, National Research Counsil of Italy, Turin, Italy.*
[10]*Independent Researcher, Ghent, Belgium.*

Summary

***Xanthomonas campestris* pv. *campestris* (Xcc) is a vascular pathogen that invades the xylem of *Brassica* crops. Current chemical and antibiotics-based control measures for this bacterium are unsustainable and inefficient. After establishing a representative collection of Xcc strains, we isolated and characterized bacteriophages from two clades of phages to assess their potential in phage-based biocontrol. The most promising phages, FoX2 and FoX6, specifically recognize (lipo) polysaccharides, associated with the *wxc* gene cluster, on the surface of the bacterial cell wall. Next, we determined and optimized the applicability of FoX2 and FoX6 in an array of complementary bioassays, ranging from seed decontamination to irrigation- and spray-based applications. Here, an irrigation-based application showed promising results. In a final proof-of-concept, a $CaCl_2$-formulated phage cocktail was shown to control the outbreak of Xcc in the open field. This comprehensive approach illustrates the potential of phage biocontrol of black rot disease in *Brassica* and serves as a reference for the broader implementation of phage biocontrol in integrated pest management strategies.**

Received 22 October, 2021; revised 4 January, 2022; accepted 5 January, 2022.
For correspondence. *E-mail jeroen.wagemans@kuleuven.be; **E-mail rob.lavigne@kuleuven.be
Microbial Biotechnology (2022) **15**(6), 1762–1782
doi:10.1111/1751-7915.14004
Funding information
This research was supported by the 'Vlaams Agentschap Innoveren en Ondernemen' (VLAIO) agriculture programme (LA) grant IWT.150914 and by the European Union's Horizon H2020 Research and Innovation Programme (grant agreement N. 773567). DH holds a predoctoral scholarship from the 'Fonds voor Wetenschappelijk Onderzoek Vlaanderen' (FWO) strategic basic research grant 1S02520N.

Introduction

The *Brassicaceae* family, also called the *Cruciferae,* contains several important crops including cabbages, kale, broccoli, oilseeds, mustard and other leafy vegetables like rocket salad. These crops have a worldwide estimated production of 70.15 million tonnes in 2019, with Asia being the largest producer (54.6 million tonnes) (FAOSTAT crops database; https://www.fao.org/faostat/en/). Their seeds are grown in temperate, coastal regions characterized by cool yet mild winters, which is crucial for flower induction in these biennial crops. In midsummer, mother lines for seed production are grown in beds and transplanted to seed production fields later on. The harvested seeds are globally distributed and primarily sold to plant nurseries (Williams, 1980; Gitaitis and Walcott, 2007; Vicente and Holub, 2013). Here, plants are grown at an industrial scale in greenhouses at very high densities. The resulting leaflings are distributed to farmers and transplanted in crop production fields. Each step of this production chain, starting from seed production to growing plants at high densities in nurseries and finally transplants in the open field, poses a potential risk to infections by phytopathogens (Holtappels *et al.*, 2021). One of the most relevant bacterial pathogens causing disease in crucifer crops is *Xanthomonas*

campestris pv. *campestris* (Xcc), causing V-shaped leaf necrosis and blackened veins, typical for black rot disease (Vicente and Holub, 2013).

Xcc is a Gram-negative, rod-shaped bacterium with a single polar flagellum. The pathogen is seed-borne, but Xcc is also known to infect crops through contaminated residues and infected weeds (Gitaitis and Walcott, 2007; Ryan *et al*., 2011; Vicente and Holub, 2013). Moreover, Xcc can grow epiphytically and infects through hydathodes or wounding of the plant (Vicente and Holub, 2013). Kamoun *et al*. (1992) were the first to recognize the existence of races within the Xcc population, which currently counts eleven established races, based on multilocus sequence typing (MLST) (Fargier and Manceau, 2007; Cruz *et al*., 2017). Whereas races 5 and 6 are more common in native crucifer weeds (Ignatov *et al*., 2007), races 1 and 4 are assumed to be most abundantly present in cultivated crucifers (Vicente *et al*., 2001).

Despite the economic impact of black rot disease in crucifers, the options to control Xcc infections remain limited. Chemical treatment of phytopathogens are generally restricted due to resistance development, soil accumulation and environmental and health concerns (Lamichhane *et al*., 2017). Moreover, the use of antibiotics in crop production is undesirable since these compounds are also prone to resistance development, influence the natural microbiota and end up in the food chain as residues (Wellington *et al*., 2013; Grenni *et al*., 2018). To address this problem, integrated pest management (IPM) has been put forward as a preferred disease management strategy (Holtappels *et al*., 2021). Within this framework, efforts are made to prevent, characterize and control the disease in a sustainable manner with respect to current cultivation techniques (Barzman *et al*., 2015).

Bacteriophages are being evaluated as alternative biocontrol agents to be integrated in IPM (Jones *et al*., 2012; Holtappels *et al*., 2021). The initial use of bacterial viruses or bacteriophages (phages) to control disease in crops dates back almost a century, when they were used in 1924 to control Xcc in cruciferous crops (Mallmann and Hemstreet, 1924; Buttimer *et al*., 2017). In recent years, the research in phage biocontrol is being revisited, driven by a better understanding of phage biology as extensively reviewed (Svircev *et al*., 2018; Holtappels *et al*., 2021; Jones *et al*., 2018).

Because of the urgent need for alternative treatment strategies for bacterial diseases, and more specifically black rot in crucifers, translational research towards the implementation of bacteriophages in practice is essential to set a standard for the overall implementation of phages as valid biocontrol agents in IPM.

In this research, we present the development of a comprehensive phage application as part of a potential future IPM approach to control *Xanthomonas campestris* pv. *campestris*. We have characterized the diversity of the Xcc population in Belgium (Flanders) using whole genome sequencing and comparing this diversity to genomes available in public databases. Furthermore, we have isolated, and characterized phages infecting Xcc and evaluated their potential taking into account microbiological traits and the disease cycle during crop production.

Results

The isolation of six Xcc-specific bacteriophages, belonging to the 'Foxunavirus' and Carpasinavirus *genera*

Fields containing brassica crops (white cabbage, red cabbage, kale, brussels sprouts, cauliflower) with typical V-shaped necrotic lesions were sampled for Xcc bacteriophage isolation. As such, a total of six lytic phages could be isolated, termed FoX (Phage of Xcc). Based on virion morphology, two clades could be distinguished: FoX1, FoX2, FoX3 and FoX5 are all myoviruses (Fig. S1A, D, E, F), while FoX6 and FoX7 have a distinct, large myovirus morphology (Fig. S1B and C).

The genomes of the six phages in the collection were determined to facilitate further selection based on the absence of potential virulence-, antibiotic resistance- or lysogeny-associated genes. The FoX1-like phages, FoX1, FoX2, FoX3 and FoX5, do not share any nucleotide sequence similarity to phage in the non-redundant NCBI database and should therefore be considered to be members of a new genus, 'Foxunavirus', as recently proposed to the International Committee on Taxonomy of Viruses. A Viptree analysis illustrated that these phages are distantly related to *Pseudomonas* phage PPpW-3 (Kawato *et al*., 2015), member of the *Jilinvirus* genus (*Myoviridae)*. Other species belonging to this genus are *Escherichia* virus ep3 and *Escherichia* virus ECO1230-10. These phages and the 'Foxunavirus' phages share a conserved genome architecture, especially in the structural and replication cassette (Fig. 1).

On average, the FoX1-related phages have a genome size of 44.8 kb and a GC content of 59%. Neither antibiotic resistance nor known virulence-associated gene was found within their genomes. Interestingly, the lysogeny cassette, and more specifically the integrase, as found in the genome of PPpW-3, is absent from the genome of either one of the 'Foxunavirus' phages, indicating a strictly lytic infection cycle, similar to *Escherichia* phage ep3 and *Escherichia* virus ECO1230-10. More details on the genome characterization and identification of the structural proteome is provided in Table S1.

The second clade contains FoX6 and FoX7, which contain genomes of 61 kb with a GC content of 52%

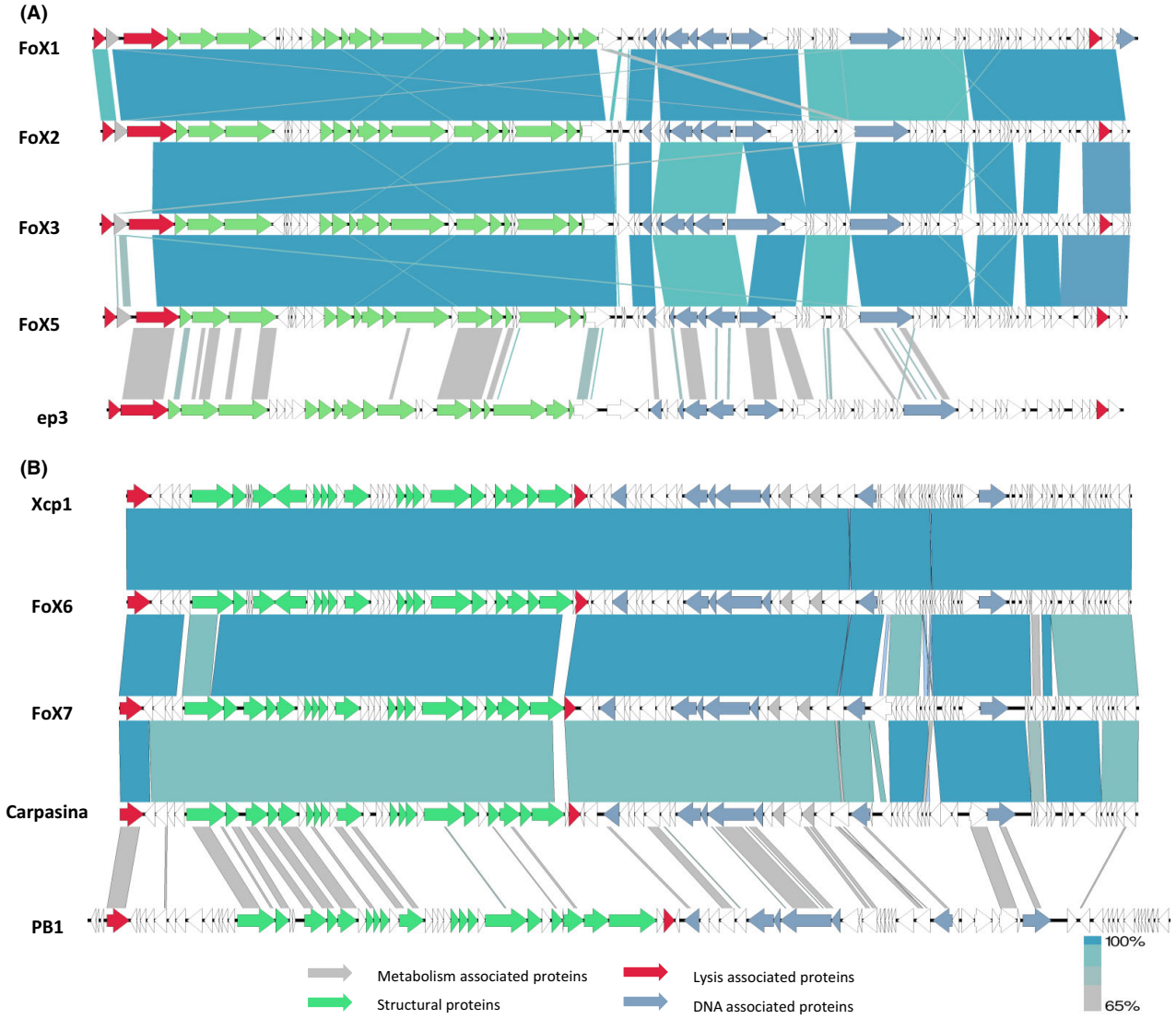

Fig. 1. Genome maps of the FoX phages.
A. Genome maps of the 'Foxunavirus' genus FoX1-like phages FoX1, FoX2, FoX3, FoX5 compared to ep3, and B. Genome maps of the *Carpasinavirus* genus FoX6-like phages FoX6 and FoX7 compared to Xcp1, Carpasina and PB1. Each arrow represents a coding sequence. In red, genes encoding lysis associated proteins, in green structural proteins, in blue DNA associated proteins and in grey enzymes involved in metabolic processes. Nucleotide sequence similarity (grey/blue scale) was predicted by a Blast similarity search (adapted from Easyfig).

and share 97% and 93% sequence identity with Xcc phages Carpasina and Xcp1, respectively. These phages are classified as members of the *Carpasinavirus* genus (*Myoviridae*) and are known to infect Xcc (Fig. 1). FoX6 and FoX7 share 99.9% sequence identity between each other, marking them as two isolates of the same species. Based on the genome annotation, no genes could be identified that potentially indicate a temperate lifestyle for these phages. Moreover, no identifiable virulence or antibiotic resistance genes were found.

A gel-free mass spectrometry analysis allowed further annotation of the virion proteins of the FoX6-like phages as 13 previously hypothetical proteins were experimentally verified as part of the virion particle (Table S2).

For both clades, a representative phage was selected for microbiological characterization. FoX2 and FoX6 were selected because they are both efficient in killing the host bacteria at a multiplicity of infection (MOI) of 0.1 and efficiently adsorb to their hosts: FoX2 has an adsorption constant of $k_{FoX2} = 4.99 \times 10^{-9}$ ml min^{-1} and 98% of phages are adsorbed after 6 min while FoX6 is less efficient with a constant of k_{FoX6} 1.6 $\times$ 10^{-8} ml min^{-1} and only 85% of phages are adsorbed after 8 min (Fig. S2).

Transposon knock-outs in Xcc lipopolysaccharide metabolism show resistance to phage infection and reduced virulence in planta

The bacterial receptors for both FoX2 and FoX6 were determined assessing their infectivity on a library of Tn5-transposon knock-out mutants from Xcc GBBC 1419 and GBBC 1412, respectively. Transposon mutagenesis resulted in an average of 270,000 transformants. This knock-out library was subsequently infected (MOI = 100) to identify for phage-resistant mutants and confirmed using drop tests (seven and five confirmed transposon mutants for FoX2 and FoX6, respectively, as summarized in Table 1. In case of FoX2, gene knock-outs in the *wxc* gene cluster showed a clear correlation to phage infectivity. This gene cluster is associated with the lipopolysaccharide (LPS) biosynthesis pathway in Xcc (Vorhölter *et al.*, 2001). Moreover, mutants lacking a sugar epimerase and polysaccharide biosynthesis proteins, were increasingly resistant to phage infection. Since these genes are also involved in exopolysaccharide production, we can reason that FoX2 additionally requires the presence of such polysaccharides to infect the host. In case of FoX6, the *wxc* gene cluster appeared to play an important role in phage infection as well. In addition, a glucose-1-phosphate thymidylyltransferase and a glucosyltranferase family 4 protein were also essential for FoX6 infection.

The resistance of the transposon knock-out mutants at the level of phage adsorption at single cell resolution was confirmed for a random subset of strains using SYBR gold-stained phages. Here, the transfer of fluorescent phage DNA was tracked over time, resulting in fluorescent bacteria only if the phage was indeed able to efficiently adsorb and transfer DNA into the bacterial cell. The efficiency of FoX2 to inject its DNA was significantly reduced when infecting the knock-out mutants. Knocking out hypothetical protein AAM40551.1 reduced the efficiency of DNA transfer from the phage particle to the cell by 60%. This effect is even more outspoken for the *wxcE* knock-out mutant, indicating that the efficiency of infection (more specifically attachment of the phage and its DNA transfer) was drastically reduced compared to the wild type (Fig. 2). The reduction of phage infectivity was most pronounced for the tested GBBC 1412 knock-out mutants, as only 5% of cells are fluorescent after phage infection.

The impact of phage resistance due to the loss of the receptor, in this case polysaccharides and LPS, on bacterial virulence was evaluated. Here, the percentage of symptomatic leaf tissue in cauliflower was calculated, plotted and compared between the different deletion mutants and the wild-type GBBC 1419 (Fig. S3). The knock-out of genes from the *wxc*-cluster did not impair the virulence of GBBC 1419 (GBBC 1419a, GBBC 1419b), although inactivation of *wxcE* had a small effect (GBBC 1419d). The strongest and significant effect is observed upon epimerase/dehydratase knock-out (GBBC 1419c – *P*-value = 0.0001).

Table 1. Summary of proteins possibly involved in FoX2 and FoX6 infection.

Phage	KO mutant	Protein	Accession number
FoX2	GBBC 1419a	Hypothetical protein	AAM40551.1
	GBBC 1419b	WxcX	CEM59621.1
	GBBC 1419c	Epimerase/ dehydratase protein	AAM41469.1
	GBBC 1419d	WxcE	CEM59621.1
	GBBC 1419e	WxcD	AAK53478.1
	GBBC 1419f	Polysaccharide biosynthesis protein	WP_011037335.1
	GBBC 1419g	Glycosyltransferase family 1 protein	WP029629050.1
FoX6	GBBC 1412a	WxcX	CEM59621.1
	GBBC 1412b	WxcD	AEL05674.1
	GBBC 1412c	Glucose-1-phosphate thymidylyltransferase	WP_006449667.1
	GBBC 1412d	Glucosyltranferase family 4 protein	WP_011035847.1
	GBBC 1412e	LPS biosynthesis protein	WP_076039015.1

Both in case of FoX2 and FoX6, proteins involved in LPS biosynthesis seem to play a major role in the infection cycle, indicating that the phages recognize LPS moieties on the outer surface of their host.

Gaining insights into the diversity of Xcc to develop a rational biocontrol strategy

Between 2011 and 2020, a collection of Xcc was established by examining diseased *Brassica* crops (*Brassica oleracea* var. *botrytis, alba, rubra, sabauda L., gemmifera, italica* and *Eruca vesicaria* ssp. *sativa*). A total of 156 symptomatic leaf samples were screened for the presence of Xcc from which 57 strains were isolated based on colony morphology and *gyrB* sequence.

A phage host range analysis performed on this collection showed that the range of the FoX1-like phages is complementary to those of FoX6 and FoX7, which have an almost identical host spectrum on the bacterial collection as established in this research (Table S3). Considering only recently and locally isolated strains, a cocktail of FoX2 and FoX6 infects 79% of the current collection efficiently (45 out of 57 strains). Historical reference strains (isolated between 1940 and 1960) for *Xanthomonas campestris* pv. *campestris, Xanthomonas campestris* pv. *armoraciae, Xanthomonas campestris* pv. *raphani, Xanthomonas campestris* pv. *barbarae* and *Xanthomonas campestris* pv. *incanae* did not show plaques when a solution of 10^6 PFU ml^{-1} was spotted.

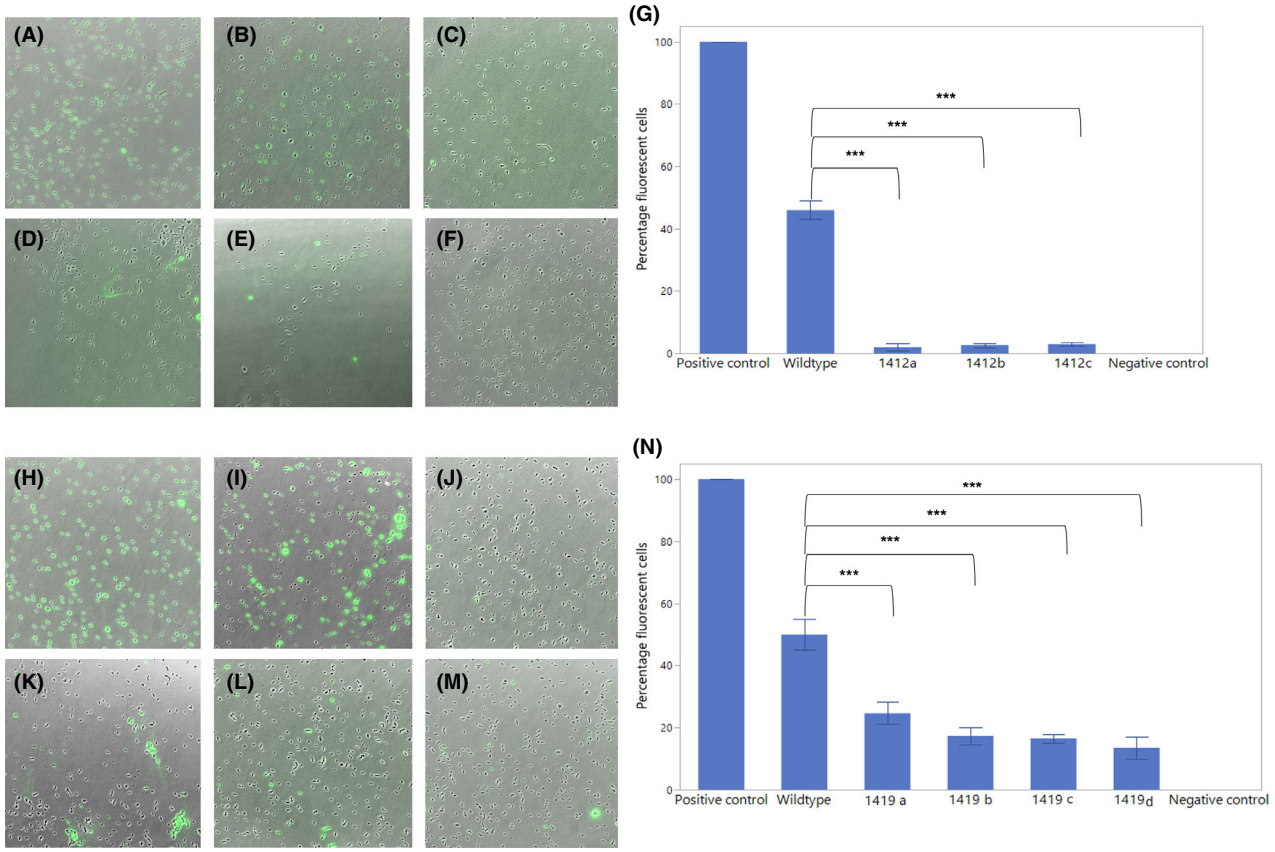

Fig. 2. Fluorescence microscopy of phage infected cells with an MOI of approximately 50.
A. GBBC 1412 stained with 0.01% SYBR Gold B.-E. GBBC 1412 (B), 1412a (C), 1412b (D) and 1412c (E) infected with SYBR Gold stained FoX6 F. GBBC 1412 without staining G. Fluorescent cell counts showed that 100% of GBBC 1412 cells are stained using 0.01% SYBR Gold while the negative control was not fluorescent. A subset of the wildtype population (45%) showed clear fluorescence when infected with 0.01% SYBR Gold labeled FoX6. In contrast, the number of fluorescent Tn5 knock-out mutants GBBC 1412a, GBBC 1412b and GBBC 1412c significantly decreased.
H. GBBC 1419 stained with 0.01% SYBR Gold I.-L. GBBC 1419 (I), 1419a (J), 1419b (K) and 1419c (L) infected with SYBR Gold stained FoX2 M. GBBC 1419 without staining N. Fluorescent cell count showing that 100% of GBBC 1419 cells were stained using 0.01% SYBR Gold while the negative control was not fluorescent. Also in this system, a portion of the wildtype population (50%) emitted a clear fluorescent signal when infected with 0.01% SYBR Gold labeled FoX2. In the transposon mutants, there is a significant reduction of the number of infected fluorescent cells compared to the wildtype GBBC 1419. Error bars illustrate the standard deviation. Asterisks indicate significance < 0.001 *P*-value.

A random subset of 24 strains were selected for whole genome sequencing and compared to an Xcc collection described by Cruz et al. (2018) using multilocus sequence analysis (MLSA) (Cruz *et al.*, 2018). This analysis proved that our collection is representative for the complete diversity within Xcc as currently described (Fig. S4). The pangenome of our Xcc collection contained 9,591 genes with 2,809 core genes present in all strains. Based on an alignment of these core genomes, our current collection supplemented with whole genome assemblies from NCBI consists of four major genome clusters (Fig. 3A). The strains isolated in the course of this project are scattered along three out of four genome clusters.

Taking into consideration the crop on which a particular strain was isolated, no direct connection between the strain diversity and the crop was observed. Nevertheless, our data suggests there is a connection between the genomic cluster and the phage susceptibility. Strains susceptible to either one of the phages appear to cluster together at the genome level, suggesting a subtle relationship between the core genome of Xcc and phage susceptibility. Interestingly, phage infectivity by either one of the two types of phages seems to strongly correlate with the genomic sequence responsible for coding the *wxc* gene cluster. More specifically, as a maximum likelihood tree shows (Fig. 3B), based on the sequence of the *wxc* gene cluster, there is a clear separation between FoX1/2- and FoX6-susceptible strains. A more in depth analysis of the full diversity of this *wxc* gene cluster suggests that there are three clusters distinguishable in the full diversity of Xcc strains available in current databases.

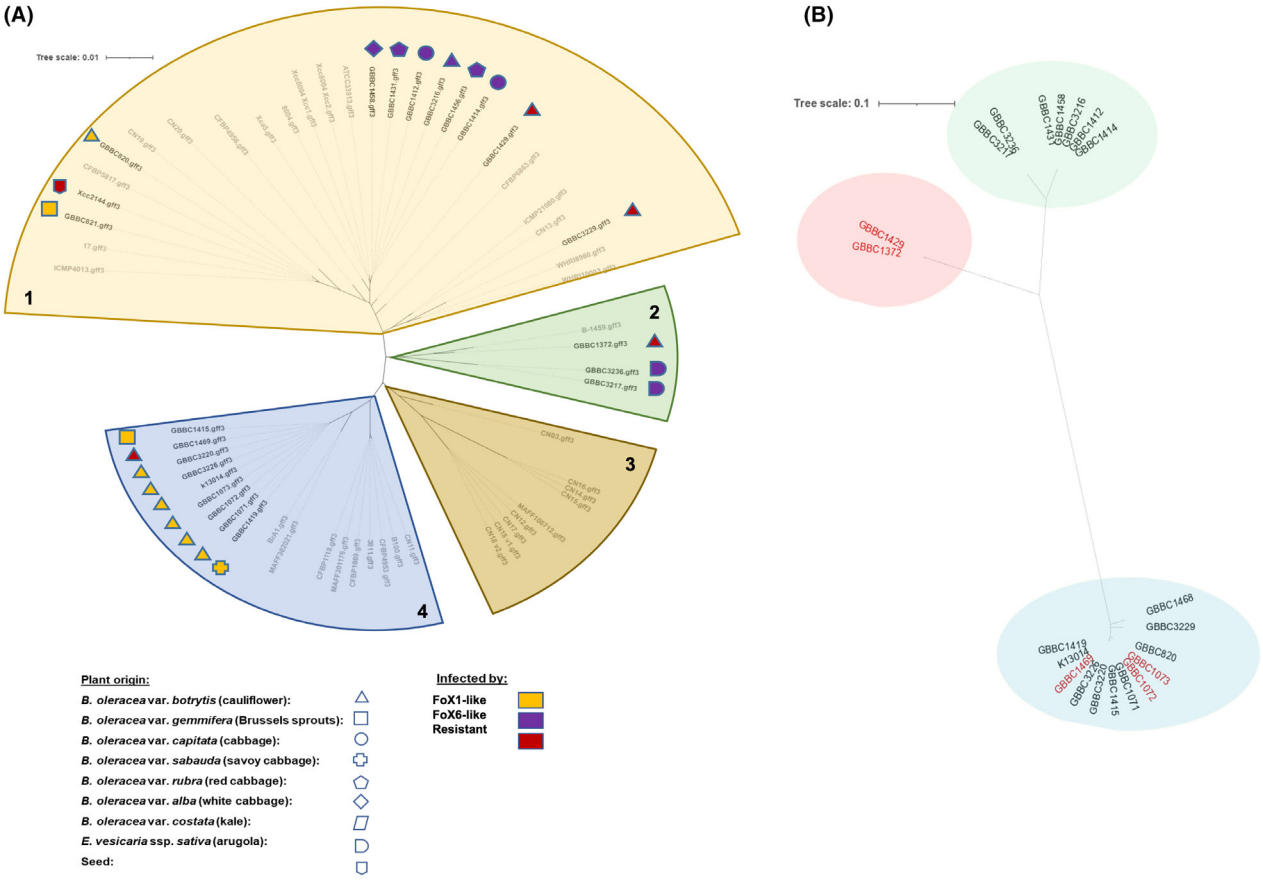

Fig. 3. A. Phylogenetic analysis of Xcc based on the core genome (2988 genes). Strains from this study are indicated in black, whereas strains from public databases are indicated in grey. Plant hosts are indicated with differently shaped icons next to the isolate's name. Colors of the icons depict the strain's susceptibility to the individual phages in collection: yellow for strains susceptible to FoX1-like phages, purple for strains that can become infected by FoX6-like phages, and red for the strains resistant the phages in our collection. Four main clusters (yellow, green, brown and blue) can be defined in the phylogeny of Xcc based on the core genome. Strains isolated in this study appear to be representative for three out of four cluster currently present in public databases.
B. Maximum likelihood tree (1000 bootstraps, Jukes-Cantor) of the wxc gene cluster of a subset of the Xcc collection. Strains in the red shape (and red font) are resistant to the phage collection, while strains in the blue and green shape are susceptible to FoX2 and FoX6, respectively.

FoX2 and FoX6 treatment reduces bacterial concentrations during seed steeping and significantly promotes the development of seedlings

The efficacy of FoX2 and FoX6 to prevent disease development by decontamination of both artificially and naturally infested seeds was evaluated. First, as Fig. 4A shows, steeping with FoX2 and FoX6 successfully reduced the number of bacteria residing on the seeds. The reduction was most pronounced when seeds were artificially infested with a bacterial load of 10^8 CFU g^{-1} and treated with an MOI of 1, resulting in a log 1.5 and log 1.7 reduction (97–98%) for FoX2 and FoX6, respectively. When infected with 10^6 CFU g^{-1} (MOI of approximately 100), the log reduction of the phage treatment slightly reduced. Finally, when the seeds were loaded with 10^4 CFU g^{-1} (MOI of approximately 10,000), the effect of the treatment dropped to a log 0.5 reduction corresponding to a 68% reduction of the initial bacterial concentration.

Next, two seed lots, naturally infected with a phage susceptible Xcc, were treated with either FoX2 or FoX6. The results obtained in this assay were comparable to the results of the artificially infected seeds. Here, a log 0.8 and log 1.2 reduction (84% and 94%) was obtained for FoX2 and FoX6, respectively (Fig. 4B). An overview of the bacterial titres is provided in Fig. S5. These data suggest that under every tested condition the majority of bacteria have been removed via phage treatment. Yet, a relevant fraction of bacteria always seemed to remain uninfected, which is possibly because a subset of the bacterial cells is not metabolically active during seed steeping. Indeed, the FoX phages were shown to not be able to infect stationary cells (Fig. S6).

The efficacy of the phages applied during steeping on disease development was evaluated by sowing the

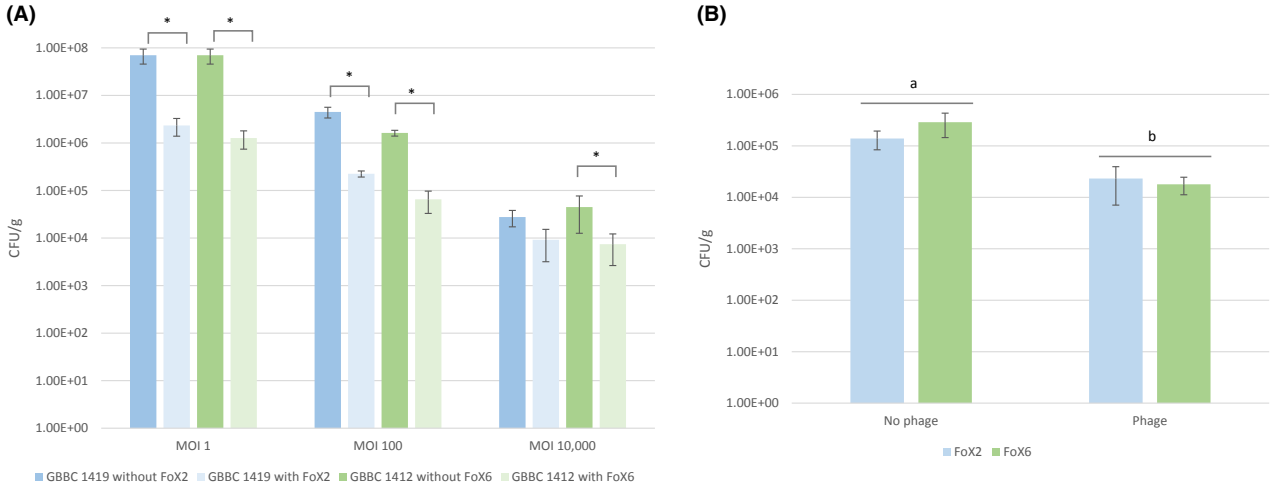

Fig. 4. Bacterial concentration (CFU g^{-1}) of Xcc after phage treatment of seeds.
A. Artificial inoculation with Xcc GBBC 1412 and GBBC 1412 treated with FoX6 and FoX2 (10^8 PFU g^{-1}), respectively. Error bars depict the standard deviation, asterisks show the level of significance (*t*-test, *P*-value < 0.05).
B. Naturally infested seeds treated with either FoX2 or FoX6 (10^8 PFU g^{-1}). Error bars depict the standard deviation, the different significance groups are indicated with a and b, *T*-test with *P*-value < 0.05).

seeds and quantifying the germination potential and growth of the seedlings. Due to differences in virulence between GBBC 1419 and GBBC 1412, parameters were measured 14 and 7 days after sowing, respectively. The phage-treated seedlings showed reduced disease symptoms and differed significantly from the non-treated seeds: both root and shoot lengths increased, while the Vigor index of the phage-treated seeds resembled the non-infected seedlings (Table 2, Fig. 5 and Fig. S7).

Efficacy of an irrigation-based phage treatment

In a next step, both FoX2 and FoX6 were evaluated in irrigation-based applications. As such, seedlings received different amounts of phages, after which the remaining phages *in planta* were quantified 14 days after phage treatment without the presence of Xcc (Fig. S8). These results indicate a minimum of 10^8 PFU/plant was required to recover 10^2 PFU/plant. Increasing the concentration tenfold resulted in an almost equal increase of phages recovered from the tissues after extensively washing the seedlings with PBS supplemented with 0.1% Tween 20.

Since the phages are able to be taken up by the plants, the efficacy of an irrigation-based phage application was tested by adding phages to young cauliflower plants over a timespan of six weeks before inoculation with Xcc. Ten days after inoculation, disease symptoms were scored, suggesting that a weekly treatment with 1×10^9 PFU of FoX2 per seedling was sufficient to significantly suppress infection by GBBC 1419, which was applied invasively by cutting the leaves with infested scissors (Fig. 6). In sharp contrast, FoX6 was unable to reduce symptoms of GBBC 1412 using a similar set-up (Fig. S9). Here, no significant differences were obtained between the positive control and either of the treatments.

Table 2. Vigour index of the seedlings after artificial infestation of the seeds with Xcc (10^6 CFU g^{-1} of GBBC 1412 and GBBC 1419, respectively) with and without phage treatment (10^9 PFU).

	Mean shoot length [cm]	Mean root length [cm]	Seed germination	Vigor index
GBBC 1412				
Negative control	3.9 (a)	5.3 (a)	100%	922 (a)
No treatment	2.5 (b)	2.3 (b)	87.5%	423 (b)
FoX6 treated	3.9 (a)	5.2 (a)	96%	876 (a)
GBBC 1419				
Negative control	5.7 (a)	6.2 (a)	100%	1191 (a)
No treatment	3.3 (b)	3.7 (c)	82%	577 (b)
FoX2 treated	5.2 (a)	4.9 (b)	91%	917 (a)

Significant differences are observed between the phage-treated object and the non-treated object (connected letter report, *P*-value < 0.05). Non-inoculated seed was taken as negative control.

Further exploration of FoX2 as a biocontrol agent shows significant reductions in symptom development in tailored bioassays

As proof of concept on the further applicability of FoX2, the phage was mixed with GBBC 1419 in a specific concentration range (MOI of 0.1, 1 and 10) and sprayed on young white cabbage plants. On average, an MOI of 10 resulted in only 15% of the leaves to be infected

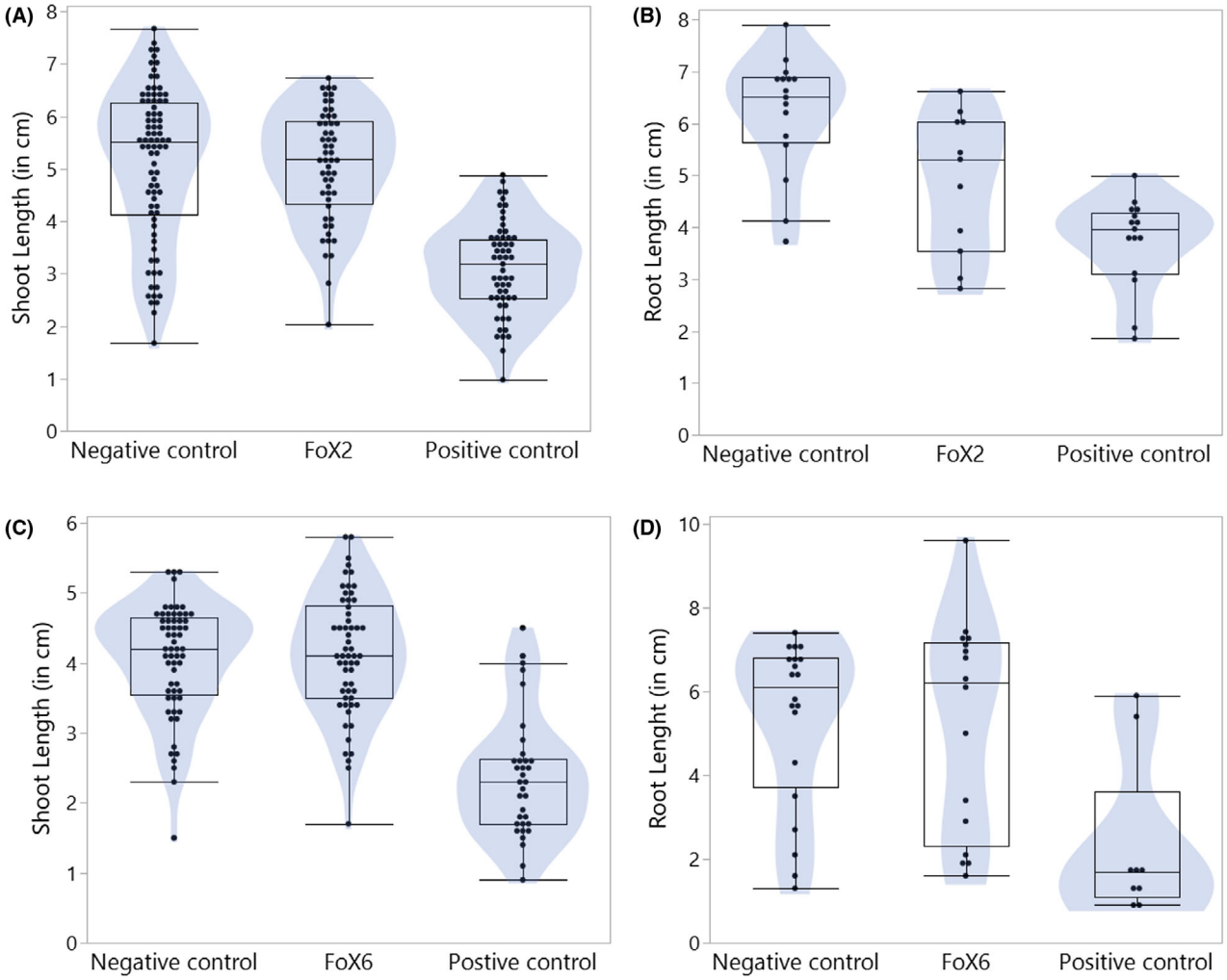

Fig. 5. Effect of phage treatment on the growth of cauliflower seedlings: negative control indicates the seedlings that were not infected and did not receive a phage treatment, positive control are seedlings that were infected (10^6 CFU g) but did not receive a phage treatment, FoX2 and FoX6 are seedlings that received a phage treatment (109 PFU) after being inoculated (10^6 CFU g^{-1}), respectively.
A.–C. Shoot length of seedlings from GBBC 1419 (A) and GBBC 1412 (C) infested seeds treated with FoX2 (A) or FoX6 (C), respectively fourteen and 7 days after sowing (n = 100). There is a significant increase of shoot length when seedlings are treated with phage (P-value of < 0.0001, Wilcoxon Kruskal/Wallis test).
B.–D. Root length of the seedlings after seed inoculation with GBBC 1419 (B) and GBBC 1412 (D), with and without FoX2 (B) and FoX6 (D) treatment, respectively fourteen and 7 days after sowing (n = 25). A significant difference is observed between the phage treated object and the positive control (P-value of 0.0083 (B) or 0.0020 (D), Wilcoxon Kruskal/Wallis test).

compared to 83% when only bacteria were sprayed (Fig. 7A and B). Also, the number of symptomatic spots per leaf, that is the entry points of the infection, were significantly different between the phage-treated leaves compared to the non-treated leaves.

A more realistic application was tested by spraying the phage (10^9 PFU ml^{-1}) prior to infection with Xcc. As such, the stability of the phage on the phyllosphere was ascertained in absence of its host. Titrations showed that 1 h after application, 10^8–10^9 PFU could be recovered per leaf, suggesting that there was no reduction in phage concentration and a homogenous application. Twenty four hours later, this concentration was reduced by 1 log unit, and after 48 h, no phages could be recovered from the leaves (Fig. S10). This demonstrates the limited stability of the viral particles on the phyllosphere in absence of the host within a greenhouse environment. Yet other factors such as plant age, the plant microbiome and irrigation probably play a crucial role in this stability as well.

Next, the efficacy of a preventive spray-based phage application demonstrated a significant reduction of the symptomatic leaf tissue after cutting the leaves with Xcc-infested scissors (10^8 CFU ml^{-1}) with medians of 1.2% and 3.1% for FoX2-treated and non-treated leaves, respectively. In a more natural inoculation set-up,

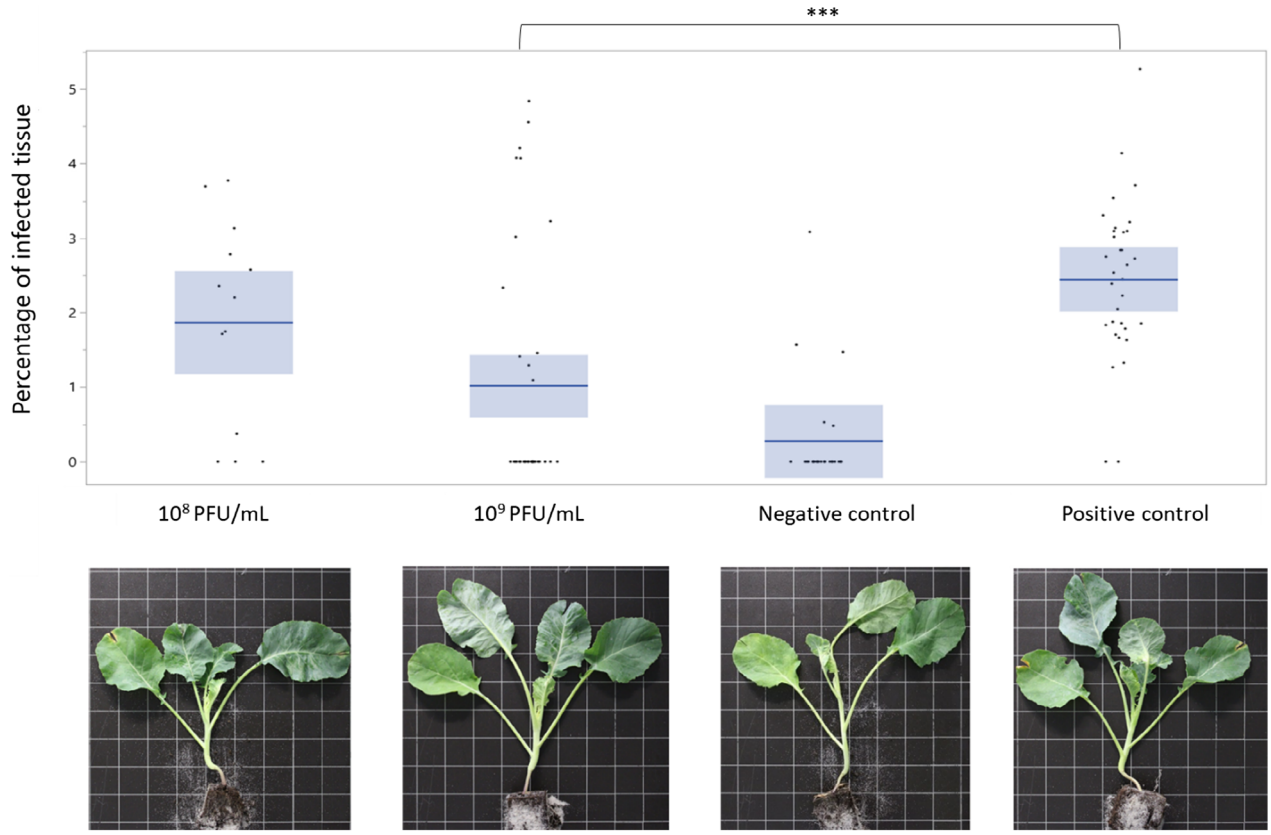

Fig. 6. Symptom development (10 days p.i. with Xcc) after irrigating a concentration gradient of phages (1 ml for 6 weeks) to young cabbage plants (n = 75 per object). Blue area plots depict the confidence interval and the blue lines represent the mean. Young cauliflower leaves were infected by cutting the tips with scissors dipped in bacterial suspension. The leaves of the positive control and the ones treated with 10^8 PFU ml^{-1} have more damaged tissue compared to leaves of the negative control (cut with sterile scissors) and leaves treated with 10^9 PFU ml^{-1}. The positive control had a median of 2.45% of the leaf surface that was infected. A treatment with 10^8 PFU ml^{-1} resulted in a median of 1.8%, while applying 10^9 PFU ml^{-1} FoX2 reduced the median of the percentage of symptomatic tissue to 0%, which is a significant reduction (P-value of 0.0002, Kruskal/Wallis test). The negative control had a median of 0% as well, indicating that there was no infection in the leaves.

cabbages were inoculated by spraying the leaves with a bacterial suspension (10^7 CFU ml^{-1}) without artificial damaging of the leaves. This resulted again in a significant symptom reduction of 34% and 40%, respectively, when phages were applied with an MOI of 10 and 100 (Fig. 7C and D) compared to the positive control. Moreover, a treatment with MOI 100 resulted in a significant decrease of the number of symptomatic entry points as well.

Field trials demonstrate the potential of the FoX2-FoX6 phage cocktail to control Xcc infection

In the summer of 2020, three independent field trials were performed on cauliflower to test the applicability of a phage cocktail consisting of FoX2 and FoX6 to control two distinct Xcc strains (GBBC 1412 and GBBC 1419). A first trial was performed in Beitem (Belgium) and resulted in a significant decrease of the number of symptomatic spots per plant (4.5 versus 7.5 spots, ten weeks post inoculation by assessment of the upper ten leaves) as summarized in Table 3. A second trial was performed in Kruishoutem (Belgium) in which calcium chloride was added to the phage cocktail to increase the adsorption of the phages to their bacterial host. Adding 2 mM of $CaCl_2$ appeared not to influence Xcc infection as illustrated by Fig. S11. The combination of the phages with $CaCl_2$ resulted in a significant decrease four weeks post inoculation of both the number of infected plants (21% versus 38%), as well as the percentage of symptomatic leaf tissue (1.70% versus 3.97%). A final trial was performed at Sint-Katelijne-Waver (Belgium), similar to the previous trial, where the number of symptoms were assessed every two weeks over a period of ten weeks. Significant differences were observed four weeks post inoculation (22% versus 39%) and after ten weeks, the number of symptomatic plants decreased to 67% compared to the non-treated object having 96% symptomatic leaves.

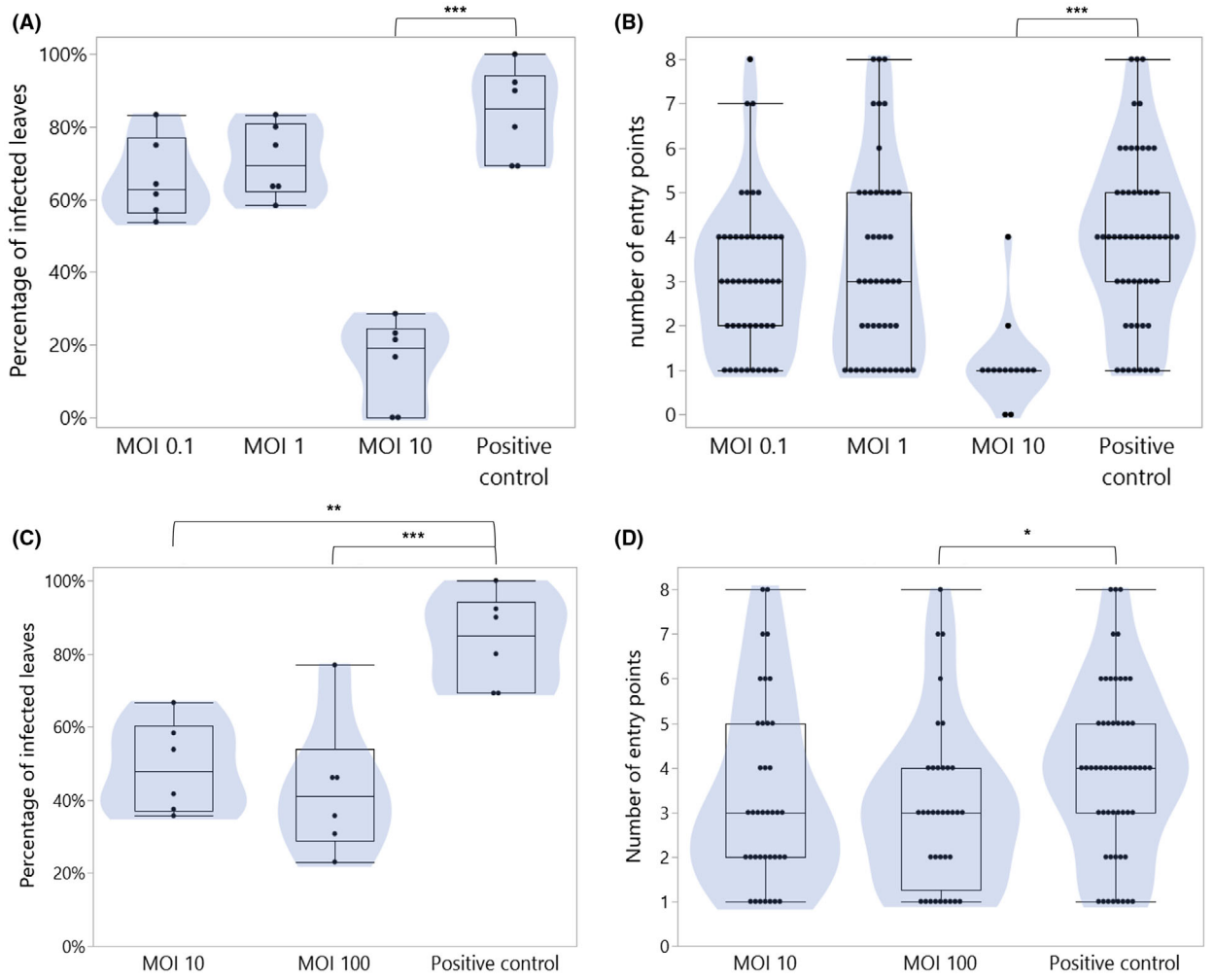

Fig. 7. A. Spray application of a mixture of phage and bacteria on cabbage plants with different multiplicity of infections (MOI 0.1, 1 and 10 – 10^7 CFU ml^{-1}). A significant reduction of the percentage of infected leaves is obtained when FoX2 is mixed with GBBC 1419 at an MOI of 10 with an average of 15% of symptomatic leaves (*P*-value of < 0.0001, *n* = 6).
B. Number of entry points counted per infected leafs 10 days after a mixture of phage and bacteria with different MOIs are applied (MOI 0.1, 1 and 10 – 10^7 CFU ml^{-1}). According to a non-parametric Wilcoxon test, there is a significant difference when FoX2 is mixed with GBBC 1419 at an MOI of 10 (*P*-value < 0.0001, *n* = 39).
C. Spray application of FoX2 (10^8 and 10^9 PFU ml^{-1}) prior to inoculation with Xcc (10^7 CFU ml^{-1}). Significant reductions of the symptomatic leaves are obtained for both an MOI of 10 and 100 (Tukey test – *P*-value 0.0032 and 0.0008, respectively, *n* = 6). However, on average, still 43 and 49% of leaves showed symptoms of Xcc.
D. Number of infection points per leaf when leaves were first treated with phage (10^8 and 10^9 PFU ml^{-1}) prior to inoculation with Xcc (10^7 CFU ml^{-1}). There is a significant difference in the number of entry points when leaves are sprayed with 10^9 PFU ml^{-1} prior to inoculation (Wilcoxon test – *P*-value 0.0178, *n* = 36).

Discussion

As most of the planet's arable surface and resources are already in use, intensifying crop cultivation is of key importance. However, pests and pathogens are a major challenge to circumvent. Hotspots of bacterial phytopathogens can have devastating effects on local food production (Savary *et al*., 2019). Overcoming these diseases and minimizing their caused yield losses is indispensable to sustain the steadily increasing human population.

Development of a representative bacterial and phage collection shows a high diversity in both bacterial host and virus

To address the problem of Xcc infections, we set up a phage-based biocontrol approach and isolated and characterized a collection of six lytic phages. FoX1, FoX2, FoX3 and FoX5 are similar to each other and make up a new species belonging to a new genus the 'Foxunavirus' genus, distantly related to the *Jilinvirus* genus. In contrast to some other phages belonging to the latter, there

Table 3. Results of the three field trials performed in this study at three different geographical locations in Belgium.

	Only Xcc	Phage cocktail	No artificial inoculation	Only Xcc	Phage cocktail	No artificial inoculation
	Percentage of infected plants			Average number of symptomatic spots per plant		
Beitem						
8 weeks p.i.	61% (ab)	79% (a)	21% (c)	8.1 (a)	7.9 (a)	1.8 (b)
10 weeks p.i.	96% (a)	100% (a)	72% (b)	7.5 (a)	4.5 (b)	1.3 (c)
	Percentage symptomatic leaves			Percentage symptomatic leaf tissue		
Kruishoutem						
4 weeks p.i.	38% (a)	21% (b)	3% (c)	3.97% (a)	1.70% (b)	0.27% (b)
Sint-Katelijne-Waver						
4 weeks p.i.	39% (a)	22% (b)	2% (c)	3% (a)	2% (b)	0% (c)
6 weeks p.i.	50% (a)	32% (b)	2% (c)	4% (a)	3% (ab)	0% (c)
8 weeks p.i.	55% (a)	30% (b)	0% (c)	5% (ab)	2% (bc)	0% (c)
10 weeks p.i.	96% (a)	67% (b)	19% (c)	10% (a)	5% (a)	1% (c)

Three conditions were tested: only inoculation with a cocktail of GBBC 1412 and GBBC 1419 (10^6 CFU ml^{-1}), inoculation with the bacterial cocktail and preventive phage application consisting of FoX2 and FoX6 (10^8 PFU ml^{-1}) supplemented with 2 mM of $CaCl_2$ and an object without inoculation of Xcc. The field trial in Beitem was assessed eight and ten weeks post inoculation (p.i.) as the percentage of infected plants in a plot and the number of symptomatic spots per plant (assessment of the top 10 leaves). In Kruishoutem (4 weeks p.i.) and Sint-Katelijne-Waver, disease was expressed as the percentage of symptomatic leaves and the percentage of symptomatic leaf tissue 4 weeks and four, six, eight and 10 weeks p.i., respectively. Significance of the data was expressed as a connecting letters report (P-value < 0.05).

are no signs of a temperate lifecycle in the FoX1-like phages, thus making them valid biocontrol candidates. Similarly to our FoX1-like phages, *Jilinvirus* members *Escherichia* virus ECO1230-10 and ep3, infecting *E. coli* responsible for bovine metritis and avian pathogenic *E. coli*, respectively, show no signs of a temperate lifestyle and have thus been proposed to be phage therapy candidates (Santos and Bicalho, 2011; Lv *et al.*, 2015).

FoX6 and FoX7 belong to the same species as Xcc phages Xcp1 and Carpasina, members of the *Carpasinavirus* genus. A phylogenetic analysis suggests that these two phages make up a third cluster within the *Pbunavirus* (Pereira da Silva *et al.*, 2019). Some *Pbunavirus* members including *Pseudomonas* viruses KTN6 and KT28 have shown biofilm-degrading properties, making them of potential use for treatment of *Pseudomonas aeruginosa* infections (Danis-Wlodarczyk *et al.*, 2015). However, no indication for this potential depolymerase activity has been observed for FoX6 nor FoX7.

One of the possible hurdles of phage biocontrol is the limited host range of the final phage cocktail. The host range of a phage can be defined as the spectrum of strains that can successfully be infected by a specific phage, meaning that the phage is able to adsorb to the bacterial cell, inject its genetic material, hijack the bacterial metabolism and produce new offspring (Hyman and Abedon, 2010). We established a bacterial collection that is considered representative for the diversity of Xcc as we cover three of the currently described genome groups as identified by a phylogenetic analysis (Cruz *et al.*, 2018). The host range of the two selected phage species is complementary to each other as the FoX1-like phages are unable to infect bacteria sensitive to FoX6-7 and vice versa.

A receptor analysis confirmed that the Xcc *wxc* gene cluster, and more specifically proteins WxcD and WxcE, is crucial for phage sensitivity. These genes are thought to be responsible for the elongation of LPS as mutants show reduced sizes of the O-antigen chain (Vorhölter *et al.*, 2001; Steffens *et al.*, 2016). In this sense, we can propose that both the FoX1-like and the FoX6-like phages recognize LPS, but FoX1-like phages also require the presence of exopolysaccharides. Accordingly, for different members of the *Carpasinavirus* genus, to which FoX6 and FoX7 belong, related to the *Pbunavirus* genus has been described that they attach to LPS in order to infect their host (Kropinski *et al.*, 1977; Garbe *et al.*, 2010; Danis-Wlodarczyk *et al.*, 2015). Because, in our case, both clades of phages appear to recognize LPS, we can further hypothesize that the bacterial strains in our collection contain differences in their LPS structure, resulting in the complementary host range as observed. Previously, comparative genomics between reference strains of Xcc illustrated that the *wxc* gene cluster is indeed divergent between the different strains (Vorhölter *et al.*, 2001; He *et al.*, 2007). As such, the authors postulated that these bacteria might have differences in their O-antigen, similar to what we observe in our phage infectivity data. LPS and more specifically the *wxc* gene cluster is considered an important virulence factor for Xcc (Qian *et al.*, 2005; Vicente and Holub, 2013). Our data further suggest that knocking out the genes encoding WxcE and an epimerase/dehydratase protein slightly reduces the virulence of Xcc. This

reduced virulence in phage-resistant mutants has previously been established for different pathosystems (Schoonejans *et al*., 1987; Filippov *et al*., 2011; Olszak *et al*., 2019; Sumrall *et al*., 2019; Holtappels *et al*., 2020). We further analysed the diversity of this *wxc* gene cluster within our strains and found that the current collection is split into three groups. Our phage infectivity data further suggests that the type of *wxc* gene cluster is determinant for a strain to be efficiently infected by either FoX1-like phage or FoX6-like phages. Recently, genomics tools based on the homology of phage receptor-binding proteins were shown to be able to predict the interaction of phages with their host on the receptor level with 45% accuracy (Gencay *et al*., 2019). This underscores the level of conservation of the interaction between phages and their host. Our genomics data further provide a rationale for a selective detection. Our current phage collection and more specifically the phage receptor-binding proteins could serve as a template for the design of phage-based detection tools to categorize the current Xcc population. Similar approaches have been published by Born and colleagues to detect the presence of phytopathogen *Erwinia amylovora* using engineered phage Y2::*luxAB* with a detection limit of 3.8×10^3 CFU ml^{-1} (Born *et al*., 2017).

Building towards a practical yet sustainable phage treatment of black rot in brassica crops

FoX2 and FoX6 were tested in bioassays using different application strategies based on current agricultural practices, taking into account the disease cycle of Xcc (Holtappels *et al*., 2021). Because Xcc is seedborne, the potential to use bacteriophages as a seed decontaminant was first evaluated. In case of artificially infected seeds, the bacterial titre dropped with 1 to 2 log units. This is in line with our previous finding for seeds infected with *Pseudomonas syringae* pv. *porri* (Holtappels *et al*., 2020). We hypothesized that the remaining fraction of bacteria are in survival mode and do not have an active metabolism that can be exploit by the phage. Our infection assay performed on stationary cells suggests that both FoX2 and FoX6 are capable of infecting the metabolically inactive cells, though with less efficiency. These data further suggest that only a minority of the phage-infected cells are producing phage progeny as theoretically all cells are infected. This is called the scavenger effect, where only phages infecting bacteria that have nutrients available are able to reproduce (Bryan *et al*., 2016). As such, during the seed bioassay, we can assume that the cells on the seeds are indeed infected, yet only a minority of the bacteria that have available nutrients are killed, explaining the limited efficacy of the treatment. During germination of seeds, nutrients come available for phage-infected bacteria, resulting in an activation of the phage that is able to complete its lytic infection cycle. This hypothesis explains the results obtained in the germination data where almost a full recovery of the seedlings is observed, seven to 14 days after sowing. Kimmelshue and colleagues showed that phages can have potential as phage-based seed coatings in controlling *Clavibacter michiganensis* subsp. *nebraskensis*. Here, the authors were able to reduce bacterial titres 76% per seed in externally infected seeds and 51% and 78% in internally infected seed in the seed and seedling tissue, respectively (Kimmelshue *et al*., 2019). On the other hand, coating of melon seeds with phage ACPWH resulted in a germination of 96% when infected with *Acidovorax citrulli* compared to 13% in non-coated seeds (Rahimi-Midani *et al*., 2020). Together, these results demonstrate the potential of phages in seed-based applications, ranging from decontamination of seeds by steeping to seed-based coatings.

In case of Xcc, another source transmission typically happens at plant nurseries. Here, seeds are sown in close proximity at ideal temperature, humidity and irrigation and later on the transplants are sold to growers (Vicente and Holub, 2013). A typical procedure used in plant nurseries is a phytodrip irrigation. In this type of irrigation, nutrients and crop protectants are preventatively fed to seeds by dripping the solution directly on the soil. As this type of application is soil- and greenhouse-based, problems with UV-sensitive phages and sunlight can be circumvented. The potential of the FoX phages in this system was further evaluated by administering a concentration gradient of phages on seeds. This experiment suggested that the minimal dose needed for the phages to remain active after 14 days was 10^8 PFU/seed. Applying tenfold more phages resulted in a tenfold increase in the recovered phage concentration. The data further suggest that the phages are indeed taken up by the seedlings, consistent with previous reports in apple, tomato and melon and are able to reduce symptom development as such (Kolozsváriné Nagy *et al*., 2015; Balogh *et al*., 2018; Rahimi-Midani and Choi, 2020). However, in our research, this application strategy was only possible to FoX2, as FoX6 was not able to prevent disease development. This underscores the importance of the individual assessment of phages for their potential in a specific application (Balogh *et al*., 2018). We further hypothesize that the phage receptor might play a role in this observation. Our data suggests that FoX2 not only needs functioning LPS metabolic genes in order to infect, but also genes involved in polysaccharide biosynthesis are crucial. This is in sharp contrast to FoX6 where these genes involved in polysaccharide production were not pinpointed during the transposon

mutagenesis. During Xcc infection, these polysaccharides play an important role in the virulence *in planta* (Wanke *et al*., 2021), potentially explaining the efficacy of FoX2 *in planta*.

The potential of FoX2 is further underpinned by the results obtained during spray applications in greenhouse conditions that show that FoX2 does have an impact on symptom development in white cabbage, though not sufficient to fully control disease development. This is attributable to the natural, limited stability of the phages on the leaf surface. Iriarte and colleagues have indeed shown that the intensity of UV light and the decline of the phage population on tomato leaves are correlated. Moreover, they have proven that also the ambient temperature influences the stability of non-formulated phage solution (Iriarte *et al*., 2007). Multiple authors have tried to circumvent these problems by adding additives to the phage solution such as sucrose, skimmed milk and other natural compounds with promising results (Born *et al*., 2015; Gašić *et al*., 2018).

Finally, our field trials demonstrate the potential of the phage cocktail to reduce symptoms in field conditions. Noteworthy, these results were obtained during a preventive application of the phage cocktail. In nature, this even distribution over a field is rare and disease manifests locally after which it spreads to neighbouring plants (Vicente and Holub, 2013). Upcoming techniques based on the principles of smart farming could contribute to a targeted application of phages to prevent the further dispersal of bacteria (Holtappels *et al*., 2021). In our system, the use of calcium chloride together with the phages reduces the number of symptomatic plants. Many phages require the presence of divalent cations like Ca^{2+} and Mg^{2+} to enhance the attachment of the phage to the bacterial host, explaining the observed effect of calcium in the field trials (Puck *et al*., 1950). Previously, our group reported a similar, subtle functionality of a phage cocktail to control *Pseudomonas syringae* pv. *porri*. In this trial, symptoms were reduced by 24.5% (S. Rombouts *et al*., 2016a). Likewise, *Xanthomonas* phage Xoo-sp2 to control *Xanthomonas oryzae* pv. *oryzae* (Xoo) reduces symptoms by one third (Dong *et al*., 2018). More profound effects were observed using Xoo phage X3 resulting in a reduction of 83.1% of the symptoms (Ogunyemi *et al*., 2019). The performance of other recent phage-based field and greenhouse trials are extensively reviewed by our group elsewhere (Holtappels *et al*., 2021). These trials demonstrate that phages have indeed a potential to be used in field-based applications, yet, the results are variable. Features such as the formulation of the phage product or environmental factors such as weather greatly influence the overall performance of the treatment.

Experimental procedures

Isolation of bacterial strains and microbiological manipulations

Xanthomonas campestris pv. *campestris* strains were isolated from symptomatic brassica crops. Leaves were surface sterilized using 70% ethanol and small pieces from the edges of symptomatic tissue were cut out and submerged in 2 ml of sterile 10-mM phosphate buffer saline (PBS). Serial dilutions were plated on Difco™ *Pseudomonas* Agar F (PAF;Becton Dickinson, Franklin Lake, NJ, USA) supplemented with 10 g l^{-1} of sucrose and incubated for 2 days at 28°C. Yellow colonies were picked and streaked three times to obtain pure cultures. Next, genomic DNA was extracted using the DNeasy Blood & Tissue kit (Qiagen, Venlo, The Netherlands). Identification of *Xanthomonas* isolates was performed by *gyrB* gene sequencing according to Parkinson *et al*., 2007 (Parkinson *et al*., 2007). Briefly, a fragment of the *gyrB* gene was PCR-amplified with the primers XgyrPCR2F (5'-AAGCAGGGCAAGAGCGAGCTGTA-3') and X.gyrrsp1 (5'-CAAGGTGCTGAAGATCTGGTC-3'), followed by Sanger sequencing. Neighbour-joining trees (bootstrap 1,000) were made using MEGA X (v6) (Kumar *et al*., 2018). After identification, bacteria were grown in lysogeny broth with reduced salt concentration (LB_{ls}) (0.5 g l^{-1} NaCl) at 25°C or on LB_{ls} solid agar plates (1.5% bacteriological agar) and 20% glycerol stocks were prepared for long-term storage at −80°C.

Isolation, characterization and production of phage collection

Xcc phages were isolated as previously published by our group (Rombouts *et al*., 2016b). In short, bacterial cultures were grown to the early exponential growth phase (OD_{600} of 0.3) in 4-ml tubes and soil (0.5 g), collected from in between the roots of the same infected crucifer crops from which the bacterial strain was isolated, was added to this culture and incubated overnight at 25°C. The mixture was centrifuged (4000 g, 10 min, 4°C), filtered using 0.45-μm syringe filters and spotted (3 μl) on a bacterial lawn of the respective host. Lysis zones were picked using a sterile toothpick and plated using the double agar technique to obtain single plaques. A single plaque was picked three subsequent times to ensure a pure phage stock. Phages were propagated as described elsewhere (Rombouts *et al*., 2016b). Due to stability issues, no chloroform was added at the end of the protocol. Transmission electron micrographs were made as described by Martino *et al*. (2021). In short, phage suspensions were absorbed for 3 min on carbon and formvar-coated copper-palladium grids,

which were then rinsed several times with water. The grids were negatively stained with aqueous 0.5% uranyl acetate and the excess fluid was removed with filter paper. Observations and photographs were made with a Philips CM10 transmission electron microscope (TEM) (Eindhoven, The Netherlands) at 80 kV. Micrograph films were developed and digitally acquired at high resolution with a D800 Nikon camera. Finally, the images were trimmed and adjusted for brightness and contrast using the Fiji software (Schindelin *et al*., 2009; Martino *et al*., 2021).

Capsid proteins were isolated starting from a PEG-precipitated phage stock ($> 10^{10}$ pfu ml^{-1}) as previously described (Wagemans *et al*., 2020). Nano-liquid chromatography-electrospray ionization tandem mass spectrometry (nanoLC-ESI-MS/MS) was used to analyse the digested samples. The peptides were identified with SEQUEST [v 1.4.0.288] (Thermo Fisher Scientific, Waltham, MA, USA) and Mascot [v 2.5] (Matrix Science, Chicago, IL, USA) based on all the predicted ORFs (Unipro UGene v1.31.1). Fast protein liquid chromatography (FPLC) was used to purify FoX2 and FoX6 on a weak anion exchanger (Diethylaminoethyl cellulose, DEAE) (CIMmultus^{TM}; BIA Separations, Ajdovscina, Slovenia) as previously published by our group (Adriaenssens *et al*., 2012).

The host range of the phages was determined by spotting (3 μL) of a dilution series (10^6 – 10^5 – 10^4 PFU ml^{-1}) on top of a bacterial lawn of the test strain, to distinguish between actual infection and lysis-from-without. If no plaques were observed at the highest phage concentration, the infection was considered highly inefficient. The infection was considered inefficient when plaques were observed at spotting 10^6 PFU ml^{-1} and efficient when plaques were observed when spotting 10^4 PFU ml^{-1}.

Phage infection *in vitro* was followed by infecting a bacterial culture (OD_{600nm} of 0.3) with MOI 1 and MOI 0.1 and following the OD_{600nm} over time using a CLARIOstar Plus system (BMG Labtech, Ortenberg, Germany). Adsorption curves were made as described previously (Holtappels *et al*., 2020).

Whole genome sequencing of bacterial and phage genomes

Bacterial DNA was extracted using the DNeasy UltraClean Microbial Kit (Qiagen) and phage DNA by a phenol/chloroform extraction (Rombouts *et al*., 2016). Bacterial and phage genomes were sequenced using an in-house Miniseq Illumina NGS platform. The Nextera Flex DNA Library Kit was used for the library prep of the DNA. FoX1, FoX3 and FoX5 were sequenced at the VIB Nucleomics core and DNA was prepared using the TruSeq library prep. The average length (700 bp) of the DNA fragments was evaluated using an Agilent Bioanalyzer 2100 and a High Sensitivity DNA Kit (Agilent Technologies, Santa Clara, CA, USA). The concentration was determined with Qubit (Thermo Fisher Scientific). Long reads were obtained using the MinION sequencer together with the MinIT (Oxford Nanopore Technologies, Oxford, UK, Flowcell R9.4.1, using the Rapid Sequencing Barcoding Kit). Illumina reads were trimmed with Trimmomatic (v0.36.5) while nanopore reads were trimmed using Porechop (v0.2.4) (Bolger *et al*., 2014; Wick *et al*., 2017a). A hybrid assembly of the genomes was obtained with Unicycler (v0.4.8.0) (Wick *et al*., 2017b) and evaluated using Bandage (v0.8.1) (Wick *et al*., 2015). Short read assemblies of the phage genomes were performed using Shovill (Seemann, 2017). Bacterial genomes were annotated using PROKKA (Seemann, 2014) and a phylogenetic tree was generated with Roary (Page *et al*., 2015). This tree was visualized by means of iTol (v4) (Letunic and Bork, 2019). MLSA was performed as described by Cruz *et al*. (2018). The phage genome ends were determined with PhageTerm (Galaxy version 1.0.11) (Garneau *et al*., 2017) and experimentally verified for the FoX1-like phages by Sanger sequencing-based primer walking. Phage genomes were annotated using the RASTtk platform (Brettin *et al*., 2015) on PATRIC (v3.6.3) pipeline (Wattam *et al*., 2017) and manually curated using BLASTp. The phages were classified according to Viptree (v1.9) and visualized using EasyFig (Sullivan *et al*., 2011; Nishimura *et al*., 2017). The genomes were checked for the presence of terminators using ARNold (Macke *et al*., 2001) and promoters using MEME (Bailey *et al*., 2009) and PHIRE (Lavigne *et al*., 2004).

Phage receptor analysis using a Tn5 knock-out mutant library and fluorescence microscopy

Phage receptors were determined as previously described (Holtappels *et al*., 2020). Briefly, a Tn5 knock-out library was made using the EZ-Tn5<KAN-2>Tnp Transposome^{TM} kit (Epicentre, Madison, WI, USA). Electrocompetent cells were electroporated (12.5 kV cm^{-1}; 25 μF; 200 Ω) (Wagemans *et al*., 2014) and plated on selective medium (50 μg ml^{-1} of kanamycin) and incubated for 2 days at 25°C. The knock-out mutants were pooled and diluted to a final concentration of 10^8 CFU ml^{-1}. To select for phage-resistant clones, the knock-out mutant library was infected at a multiplicity of infection (MOI) of 50. Phage-resistant colonies were picked, grown in liquid selective medium and re-evaluated for their resistance by spotting 5×10^7 PFU on top of a bacterial lawn containing the presumable phage resistant clone and DNA was extracted using the GeneJET Genomic DNA Purification Kit (Thermo Fisher Scientific). The location of the transposon inside the genome of the phage-resistant clones was determined by

means of a TAIL-PCR and analysed using tBLASTx (States and Gish, 1994; Singer and Burke, 2003).

Phage adsorption was evaluated using fluorescence microscopy according to Kunisaki and Tanji (Kunisaki and Tanji, 2010). In short, phages were fluorescently labelled using SYBR Gold by mixing a 10,000 times diluted fluorescent dye solution with a PEG-precipitated phage stock of 10^{11} PFU ml^{-1}. The mixture was incubated for 16 h at 4°C in total darkness. Fluorescently labelled phages were concentrated using Amicon® ultra centrifugal filters with a 30 kDa cut-off. The pellet was washed three times with phage buffer (10 mM of Tris/HCl, 10 mM of $MgSO_4$, 150 mM of NaCl, pH 7.5). Adsorption assays were performed by infecting a bacterial culture at OD_{600} of 0.1 with a multiplicity of infection equal to 50. Microscopy experiments were performed by first placing cells and/or phages between AB agar pads (AB minimal medium (0.2% $(NH_4)_2SO_4$, 0.6% Na_2HPO_4, 0.3% KH_2PO_4, 0.3% NaCl, supplemented with 0.1 mM of $CaCl_2$, 1 mM of $MgCl_2$, 0.003 mM of $FeCl_3$, 0.2% glucose and 0.25% glycerol and 1,5% agarose) and a cover glass using Gene Frames (Thermo Fisher Scientific). For imaging, a Ti-Eclipse inverted microscope (Nikon, Champigny-sur-Marne, France) equipped with a 60× Plan Apo λ oil objective, a TI-CT-E motorized condenser and a Nikon DS-Qi2 camera was used. SYBR Gold was visualized using a quad-edge dichroic (395/470/550/640 nm) and a FITC single emission filter in combination with a SpectraX LED illuminator (Lumencor, Beaverton, OR, USA) as light source, using the 470/24 excitation filter. Image data were acquired using the NIS-Elements software platform (Nikon) and the resulting pictures were further analysed using the ImageJ open source software (Schneider *et al.*, 2012).

Virulence assay of transposon knock-out mutants

White cabbage plants (*Brassica alba*) at BBCH6 were infected with the transposon knock-out mutants by cutting three leaves per plant randomly with infected scissors submerged in a bacterial solution of OD_{600nm} of 0.1 (five plants in total). The plants were covered with transparent plastic boxes for 7 days to maintain a high humidity. Ten days after infection, symptom development was quantified by calculating the percentage of infected tissue by measuring the area of the V-shaped necrosis and dividing this by the total leaf area. Statistical analysis was performed using the JMP Pro 15 software.

Seed bioassay using artificially and naturally infected cauliflower seeds

A seed bioassay was performed as described before, with minor modifications (Holtappels *et al.*, 2020). In short, cauliflower seeds (Giewont; Seminis, Saint Louis, MI, USA) were sterilized using 5% hypochlorite, rinsed with sterile mQ water and dried for 1 h in a laminar flow cabinet. Next, the seeds were incubated in a bacterial suspension (GBBC 1412 or GBBC 1419) for 2 h and again dried for 1 h under a laminar flow resulting in a final concentration of 10^8–10^6–10^4 CFU g^{-1} seed. Sterile and infected seeds were steeped by shaking them at 16°C for 18 h in sterile mQ water in six independent steeping set-ups. Phages were added at a final concentration of 10^8 PFU ml^{-1}. Both phage and bacterial titres were monitored by homogenizing 0.3 g (in six-fold) seeds in 1 ml of PBS and plating the final suspension on semi-selective brilliant cresyl blue-starch (BS) medium (Mulrean and Schroth, 1980). The remaining seeds (up to 100 seeds) were sterilely sown on 1/4th of Murashige and Skoog medium supplemented with 10 g l^{-1} Phytagel® and grown at 16°C with a 16/8 day/night regime and evaluated seven (GBBC 1412-infected seeds) or 14 (GBBC 1419-infected seeds) days after sowing. Naturally contaminated seed was processed similarly.

Infection on stationary cells was evaluated by infecting an overnight culture (OD_{600nm} of 1) with 10^8 PFU ml^{-1} of either FoX2 or FoX6. Every hour, an aliquot was taken and bacterial cells were removed (in case of FoX2 by chloroform treatment, in case of FoX6 by centrifugation) and placed on ice for further processing. The phage suspension was plated using an agar overlay to quantify the phage concentration.

Irrigation-based bioassay

The efficacy of an irrigation-based phage treatment was evaluated on Cauliflower Clarina (Syngenta, Basel, Switzerland). In total, 150 seeds were treated with 1 ml of 10^8 or 10^9 PFU ml^{-1} phage cocktail consisting of FoX2 and FoX6. The plants were grown for six weeks and treated weekly with the same dosage of phage. Twenty-four hours after the last treatment, up to four leaves per plant and 10 plants per condition, were infected by cutting the leaves with contaminated scissors with either GBCC 1412 or GBBC 1419. The plants were kept in high humidity for 10 days. The infected area was calculated and the percentage of infected leaf tissue was determined. Statistical analysis was performed using the JMP Pro 15 software.

The concentration of phages taken up by cabbage seedlings was evaluated by adding 1 ml of phages to freshly sown seeds. After 2 weeks, seedlings were harvested and washed three times in sterile mQ supplemented with 0.1% Tween 20. Seedlings were crushed with a pestle and mortar and suspended in 1 ml of PBS buffer. The phage concentration per seedling was determined by plating a dilution series. Eight seedlings were

evaluated and the experiment was repeated in five repeats.

Small-scale bioassays of FoX phages on young white cabbage plants

The applicability of FoX2 to infect GBBC 1419 was tested in a greenhouse environment. The bacteria and phage were mixed in different concentrations (10^7 CFU ml^{-1} with 10^6, 10^7 and 10^8 PFU ml^{-1} supplemented with 0.025% Silwet Gold) and sprayed over young white cabbage plants (two independent repeats, three plants per repeat). After application of the bacteria-phage cocktail, the plants were covered for 14 days underneath transparent plastic boxes to keep the plants a high humidity. Infection was assessed by counting the number of infected leaves per plant together with the total number of leaves. The severity of infection was estimated by counting the number of infection points per leaf visible as V-shaped necrotic tissue.

To test the stability of the phages in the phyllosphere in a greenhouse environment, FoX2 at $1x10^9$ PFU ml^{-1} (supplemented with 0.025% Silwet Gold) was sprayed over young cabbage plants ($n = 75$) in five independent repeats. Four leaves per object were randomly sampled 1, 24 and 48 h after treatment. Each leaf was shaken for 24 h at 4°C in 10 ml of PBS supplemented with 0.1% Tween 20 to extract phages from the leaf surface. This suspension was filtered (0.45 μm) and the phage concentration was titred.

A preventive phage treatment with FoX2 was tested on young white cabbage leaflings by applying a concentration of 10^8 or 10^9 PFU ml^{-1}. Infection with Xcc GBBC 1419 was performed by spraying a bacterial suspension (10^7 CFU ml^{-1}, 0.025% Silwet Gold) 30 min after the phage application (when the leaves were dried). Both assays were performed in two independent repeats with three plants. The efficacy of the treatment was evaluated by counting the number of infected leaves per plant and the number of entry points per infected leaf, 14 days after infection.

The effect of 2 mM of CaCl2 on Xcc infection was evaluated using a bacterial suspension of both GBBC 1412 and GBBC 1419 at a concentration of 10^6 CFU ml^{-1} supplemented with 0.025% Silwet Gold in duplicate (in total 30 plants were used). The suspension was sprayed on the cauliflower leaflings (25 ml for 12 plants). The plants were covered with transparent plastic containers for 10 days. The number of infected leaves as well as the number of infection sites was quantified.

Field trials

In total, three field trials have been performed at three different geographical locations in Belgium: Kruishoutem (N 50.94337°, E 3.52710°), Sint-Katelijne-Waver (N 51.078120°, E 4.528180°) and Beitem (N 50.901508°, E 3.124464°). Kruishoutem is characterized by a sandy soil, Beitem by a sandy-loam soil type and have a maritime climate with mild winters and cool summers. Sint-Katelijne-Waver is situated in the center of Flanders and has slightly warmer summers and cooler winters and a sandy-loam soil type. The amount of rainfall is slightly higher at Kruishoutem and Beitem compared to Sint-Katelijne-Waver.

The field trial performed in Beitem was conducted on cauliflower (Giewont). Leaflings (six-weeks-old, forty plants per object) were planted midsummer and were infected after 6 weeks by spraying a cocktail of Xcc GBBC 1412 and GBBC 1419 at a concentration of 10^6 CFU ml^{-1} at 1000 l ha^{-1}. The plants were covered for 48 h to allow an efficient infection. Twelve days after infection, a cocktail of FoX2 and FoX6 was sprayed at a concentration of 10^8 PFU ml^{-1} at 500 l ha^{-1}. The treatment was repeated three times with an interval of 7 days. The treatment was assessed based on the percentage of infected plants and the number of necrotic spots per plant counted on the upper ten leaves, eight and ten weeks post infection.

The second field trial at Kruishoutem was performed on cauliflower (Giewont) (eight-weeks-old plants) as well during midsummer. Six weeks after planting, a cocktail of FoX2 and FoX6 (10^8 PFU ml^{-1}) was sprayed in addition of 2 mM of $CaCl_2$ at 500 l ha^{-1}. One day after the first phage treatment, the plants were infected analogously to the first field trial in Beitem (cocktail of Xcc GBBC 1412 and GBBC 1419, 10^6 CFU ml^{-1}). The phage treatment was repeated four times with intervals of 1 week. An endpoint measurement was performed assessing the percentage of symptomatic leaves and the percentage of symptomatic leaf tissue four weeks post infection.

A final trial was performed in Sint-Katelijne-Waver using cauliflower (Clarina) (four-weeks-old) in midsummer. The plants were treated weekly for 3 months similarly as the second trial and the infection occurred one day after the first phage treatment (cocktail of Xcc GBBC 1412 and GBBC 1419, 10^6 CFU ml^{-1}). The cauliflowers were scored intermediately every two weeks determining the percentage of infected leaves and the percentage of infected leaf tissue.

Data analysis was performed using the 'Agriculture Research Management' (ARM) software and ANOVA.

Acknowledgements

The authors thank A. Volckaert for her input, Dr. L. van der Heijden (Bejo Zaden B.V.), Ms. K. Sereti (Rijk Zwaan Zaadteelt en zaadhandel B.V.) for providing seed

material and Prof. L. Cruz for providing us with a well-characterized Xcc collection. They further thank Miss Y. Busschots for her technical assistance.

This research was supported by the 'Vlaams Agentschap Innoveren en Ondernemen' (VLAIO) agriculture programme (LA) grant IWT.150914 and by the European Union's Horizon H2020 Research and Innovation Programme (grant agreement N. 773567). DH holds a predoctoral scholarship from the 'Fonds voor Wetenschappelijk Onderzoek Vlaanderen' (FWO) strategic basic research grant 1S02520N.

Author contributions

D.H., M.M., J.V.V., R.L. and J.W. designed the research plan; D.H., K.F., L.M., N.B., L.B., S.V., S.R., L.L., S.B., S.P., J.N., F.O., M.V. performed the experiments; D.H. wrote the first draft of this manuscript; all authors reviewed and corrected the manuscript.

Conflict of interest

The authors declare that there are no competing interest.

Data availability statement

The genomes of the FoX phages can be accessed through accession numbers MT161381, MT161382, MT161383, MT161384, MT161386 and MT161387 (NCBI). The data have been deposited with links to BioProject accession number PRJNA729255 in the NCBI BioProject database (https://www.ncbi.nlm.nih.gov/bioproject/).

References

Adriaenssens, E.M., Lehman, S.M., Vandersteegen, K., Vandenheuvel, D., Philippe, D.L., Cornelissen, A., *et al*. (2012) CIM® monolithic anion-exchange chromatography as a useful alternative to CsCl gradient purification of bacteriophage particles. *Virology* **434:** 265–270.

Bailey, T.L., Boden, M., Buske, F.A., Frith, M., Grant, C.E., Clementi, L., *et al*. (2009) MEME SUITE: tools for motif discovery and searching. *Nucleic Acids Res* **37:** W202–W208.

Balogh, B., Nga, N.T.T., and Jones, J.B. (2018) Relative level of bacteriophage multiplication in vitro or in phyllosphere may not predict in planta efficacy for controlling bacterial leaf spot on tomato caused by *Xanthomonas perforans*. *Front Microbiol* **9:** 2176.

Barzman, M., Bàrberi, P., Birch, A.N.E., Boonekamp, P., Dachbrodt-Saaydeh, S., Graf, B., *et al*. (2015) Eight principles of integrated pest management. *Agron Sustain Dev* **35:** 1199–1215.

Bolger, A.M., Lohse, M., and Usadel, B. (2014) Trimmomatic: a flexible trimmer for Illumina sequence data. *Bioinformatics* **30:** 2114–2120.

Born, Y., Bosshard, L., Duffy, B., Loessner, M.J., and Fieseler, L. (2015) Protection of Erwinia amylovora bacteriophage Y2 from UV-induced damage by natural compounds. *Bacteriophage* **5:** e1074330.

Born, Y., Fieseler, L., Thony, V., Leimer, N., Duffy, B., and Loessner, M.J. (2017) Engineering of bacteriophages Y2: dpoL1-C and Y2:luxAB for efficient control and rapid detection of the fire blight pathogen, Erwinia amylovora. *Appl Environ Microbiol* **83:** e00341-17.

Brettin, T., Davis, J.J., Disz, T., Edwards, R.A., Gerdes, S., Olsen, G.J., *et al*. (2015) RASTtk: a modular and extensible implementation of the RAST algorithm for building custom annotation pipelines and annotating batches of genomes. *Sci Rep* **5:** 1–6.

Bryan, D., El-Shibiny, A., Hobbs, Z., Porter, J., and Kutter, E.M. (2016) Bacteriophage T4 infection of stationary phase *E. coli*: life after log from a phage perspective. *Front Microbiol* **7:** 1–12.

Buttimer, C., McAuliffe, O., Ross, R.P., Hill, C., O'Mahony, J., and Coffey, A. (2017) Bacteriophages and bacterial plant diseases. *Front Microbiol* **8:** 1–15.

Cruz, J., Tenreiro, R., and Cruz, L. (2017) Assessment of diversity of *Xanthomonas campestris* pathovars affecting cruciferous plants in Portugal and disclosure of two novel *X. campestris* pv. *campestris* races. *J Plant Pathol* **99:** 403–414.

Cruz, J., Tenreiro, R., and Cruz, L. (2018) Inference of the phylogenetic diversity and population structure of *Xanthomonas campestris* affecting Brassicaceae using a multilocus sequence typing-based approach. *Plant Pathol* **67:** 948–956.

Danis-Wlodarczyk, K., Olszak, T., Arabski, M., Wasik, S., Majkowska-Skrobek, G., Augustyniak, D., *et al*. (2015) Characterization of the newly isolated lytic bacteriophages KTN6 and KT28 and their efficacy against *Pseudomonas aeruginosa* biofilm. *PLoS One* **10:** 1–20.

Dong, Z., Xing, S., Liu, J., Tang, X., Ruan, L., Sun, M., *et al*. (2018) Isolation and characterization of a novel phage Xoo-sp2 that infects *Xanthomonas oryzae* pv. *oryzae*. *J Gen Virol* **99:** 1453–1462.

Fargier, E., and Manceau, C. (2007) Pathogenicity assays restrict the species *Xanthomonas campestris* into three pathovars and reveal nine races within *X. campestris* pv. *campestris*. *Plant Pathol* **56:** 805–818.

Filippov, A.A., Sergueev, K.V., He, Y., Huang, X.-Z., Gnade, B.T., Mueller, A.J., *et al*. (2011) Bacteriophage-resistant mutants in yersinia pestis: identification of phage receptors and attenuation for mice. *PLoS One* **6:** 1–11.

Garbe, J., Wesche, A., Bunk, B., Kazmierczak, M., Selezska, K., Rohde, C., *et al*. (2010) Characterization of JG024, a *Pseudomonas aeruginosa* PB1-like broad host range phage under simulated infection conditions. *BMC Microbiol* **10:** 301.

Garneau, J.R., Depardieu, F., Fortier, L.C., Bikard, D., and Monot, M. (2017) PhageTerm: a tool for fast and accurate determination of phage termini and packaging mechanism using next-generation sequencing data. *Sci Rep* **7:** 1–10.

Gašić, K., Kuzmanović, N., Ivanović, M., Prokić, A., Šević, M., and Obradović, A. (2018) Complete genome of the *Xanthomonas euvesicatoria* specific bacteriophage KΦ1, its survival and potential in control of pepper bacterial spot. *Front Microbiol* **9:** 1–12.

Gencay, Y.E., Gambino, M., Prüssing, T.F., and Brøndsted, L. (2019) The genera of bacteriophages and their

receptors are the major determinants of host range. *Environ Microbiol* **21:** 2095–2111.
Gitaitis, R., and Walcott, R. (2007) The epidemiology and management of seedborne bacterial diseases. *Annu Rev Phytopathol* **45:** 371–397.
Grenni, P., Ancona, V., and Barra Caracciolo, A. (2018) Ecological effects of antibiotics on natural ecosystems: a review. *Microchem J* **136:** 25–39.
He, Y.-Q., Zhang, L., Jiang, B.-L., Zhang, Z.-C., Xu, R.-Q., Tang, D.-J., *et al*. (2007) Comparative and functional genomics reveals genetic diversity and determinants of host specificity among reference strains and a large collection of Chinese isolates of the phytopathogen *Xanthomonas campestris* pv. *campestris*. *Genome Biol* **8:** 1–26.
Holtappels, D., Fortuna, K., Lavigne, R., and Wagemans, J. (2021) The future of phage biocontrol in integrated plant protection for sustainable crop production. *Curr Opin Biotechnol* **68:** 60–71.
Holtappels, D., Kerremans, A., Busschots, Y., Van Vaerenbergh, J., Maes, M., Lavigne, R., and Wagemans, J. (2020) Preparing for the KIL: receptor analysis of *Pseudomonas syringae* pv. *porri* phages and their impact on bacterial virulence. *Int J Mol Sci* **21:** 1–15.
Hyman, P., and Abedon, S.T. (2010) Bacteriophage host range and bacterial resistance. *Adv Appl Microbiol* **70:** 217–248.
Ignatov, A., Sechler, A., Schuenzel, E.L., Agarkova, I., Oliver, B., Vidaver, A.K., and Schaad, N.W. (2007) Genetic diversity in populations of *Xanthomonas campestris* pv. *campestris* in cruciferous weeds in central coastal California N. *Phytopathology* **97:** 803–812.
Iriarte, F.B., Balogh, B., Momol, M.T., Smith, L.M., Wilson, M., and Jones, J.B. (2007) Factors affecting survival of bacteriophage on tomato leaf surfaces. *Appl Environ Microbiol* **73:** 1704–1711.
Jones, J.B., Svircev, A.M., and Obradović, A.Ž. (2018) Crop use of bacteriophages. In *Bacteriophages*. Harper, D., Abedon, S., Burrowes, B., McConville, M. (eds). Cham, Switzerland: Springer, pp. 839–856.
Jones, J.B., Vallad, G.E., Iriarte, F.B., Obradović, A., Wernsing, M.H., Jackson, L.E., *et al*. (2012) Considerations for using bacteriophages for plant disease control. *Bacteriophage* **2:** 208–214.
Kamoun, S., Tola, E., Kamdar, H., and Kado, C.I. (1992) Rapid generation of directed and unmarked deletions in Xanthomonas. *Mol Microbiol* **6:** 809–816. doi: 10.1111/j.1365-2958.1992.tb01531.x.
Kawato, Y., Yasuike, M., Nakamura, Y., Shigenobu, Y., Fujiwara, A., Sano, M., and Nakai, T. (2015) Complete genome sequence analysis of two *Pseudomonas plecoglossicida* phages, potential therapeutic agents. *Appl Environ Microbiol* **81:** 874–881.
Kimmelshue, C., Goggi, A.S., and Cademartiri, R. (2019) The use of biological seed coatings based on bacteriophages and polymers against *Clavibacter michiganensis* subsp. *nebraskensis* in maize seeds. *Sci Rep* **9:** 1–11.
Kolozsváriné Nagy, J., Schwarczinger, I., Künstler, A., Pogány, M., and Király, L. (2015) Penetration and translocation of Erwinia amylovora-specific bacteriophages in apple - a possibility of enhanced control of fire blight. *Eur J Plant Pathol* **142:** 815–827.
Kropinski, A.M., Chan, L., Jarrell, K., and Milazzo, F.H. (1977) The nature of *Pseudomonas aeruginosa* strain PAO bacteriophage receptors. *Can J Microbiol* **23:** 653–658.
Kumar, S., Stecher, G., Li, M., Knyaz, C., and Tamura, K. (2018) MEGA X: molecular evolutionary genetics analysis across computing platforms. *Mol Biol Evol* **35:** 1547–1549.
Kunisaki, H., and Tanji, Y. (2010) Intercrossing of phage genomes in a phage cocktail and stable coexistence with *Escherichia coli* O157:H7 in anaerobic continuous culture. *Appl Microbiol Biotechnol* **85:** 1533–1540.
Lamichhane, J.R., Bischoff-Schaefer, M., Bluemel, S., Dachbrodt-Saaydeh, S., Dreux, L., Jansen, J.-P., *et al*. (2017) Identifying obstacles and ranking common biological control research priorities for Europe to manage most economically important pests in arable, vegetable and perennial crops. *Pest Manag Sci* **73:** 14–21.
Lavigne, R., Sun, W.D., and Volckaert, G. (2004) PHIRE, a deterministic approach to reveal regulatory elements in bacteriophage genomes. *Bioinformatics* **20:** 629–635.
Letunic, I., and Bork, P. (2019) Interactive Tree Of Life (iTOL) v4: recent updates and new developments. *Nucleic Acids Res* **47:** W256–W259.
Lv, M., Wang, S., Yan, G., Sun, C., Feng, X., Gu, J., *et al*. (2015) Genome sequencing and analysis of an *Escherichia coli* phage vB_EcoM-ep3 with a novel lysin, Lysep3. *Virus Genes* **50:** 487–497.
Macke, T.J., Ecker, D.J., Gutell, R.R., Gautheret, D., Case, D.A., and Sampath, R. (2001) RNAMotif, an RNA secondary structure definition and search algorithm. *Nucleic Acids Res* **29:** 4724–4735.
Mallmann, W., and Hemstreet, C. (1924) Isolation of an inhibitory substance from plants. *Agric Res* **28:** 599–602.
Martino, G., Holtappels, D., Vallino, M., Chiapello, M., Turina, M., Lavigne, R., et al. (2021) Molecular Characterization and Taxonomic Assignment of Three Phage Isolates from a Collection Infecting.
Mulrean, E.N., and Schroth, M.N. (1980) A semiselective medium for the isolation of *Xanthomonas campestris* pv. *juglandis* from walnut buds and catkins. *Phytopathology* **71:** 336–339.
Nishimura, Y., Yoshida, T., Kuronishi, M., Uehara, H., Ogata, H., and Goto, S. (2017) ViPTree: the viral proteomic tree server. *Bioinformatics* **33:** 2379–2380.
Ogunyemi, S.O., Chen, J., Zhang, M., Wang, L.I., Masum, M.M.I., Yan, C., *et al*. (2019) Identification and characterization of five new OP2-related Myoviridae bacteriophages infecting different strains of *Xanthomonas oryzae* pv. *oryzae*. *J Plant Pathol* **101:** 263–273.
Olszak, T., Danis-Wlodarczyk, K., Arabski, M., Gula, G., Maciejewska, B., Wasik, S., *et al*. (2019) Pseudomonas aeruginosa PA5oct jumbo phage impacts planktonic and biofilm population and reduces its host virulence. *Viruses* **11:** 1–20.
Page, A.J., Cummins, C.A., Hunt, M., Wong, V.K., Reuter, S., Holden, M.T.G., *et al*. (2015) Roary: rapid large-scale prokaryote pan genome analysis. *Bioinformatics* **31:** 3691–3693.
Parkinson, N., Aritua, V., Heeney, J., Cowie, C., Bew, J., and Stead, D. (2007) Phylogenetic analysis of

Xanthomonas species by comparison of partial gyrase B gene sequences. *Int J Syst Evol Microbiol* **57:** 2881–2887.

Pereira da Silva, F., da Silva Xavier, A., Prieto Bruckner, F., Reis de Rezende, R., Pereira Vidigal, P.M., and Alfenas-Zerbini, P. (2019) Biological and molecular characterization of a bacteriophage infecting *Xanthomonas campestris* pv. *campestris*, isolated from brassica fields. *Arch Virol* **164:** 1857–1862.

Puck, B.Y.T.T., Garen, A., and Cline, J. (1950) The mechanism of virus attachment to host cells. *J Exp Me* **93:** 65–88.

Qian, W., Jia, Y., Ren, S.X., He, Y.Q., Feng, J.X., Lu, L.F., *et al*. (2005) Comparative and functional genomic analyses of the pathogenicity of phytopathogen *Xanthomonas campestris* pv. *campestris*. *Genome Res* **15:** 757–767.

Rahimi-Midani, A., and Choi, T.-J. (2020) Transport of phage in melon plants and inhibition of progression of bacterial fruit blotch. *Viruses* **12:** 1–9.

Rahimi-Midani, A., Kim, J.O., Kim, J.H., Lim, J., Ryu, J.G., Kim, M.K., and Choi, T.J. (2020) Potential use of newly isolated bacteriophage as a biocontrol against *Acidovorax citrulli*. *Arch Microbiol* **202:** 377–389.

Rombouts, S., Van Vaerenbergh, J., Volckaert, A., Baeyen, S., De Langhe, T., Declercq, B., *et al*. (2016a) Isolation and characterization of *Pseudomonas syringae* pv. *porri* from leek in Flanders. *Eur J Plant Pathol* **144:** 185–198.

Rombouts, S., Volckaert, A., Venneman, S., Declercq, B., Vandenheuvel, D., Allonsius, C.N., *et al*. (2016) Characterization of novel bacteriophages for biocontrol of bacterial blight in leek caused by *Pseudomonas syringae* pv. *porri*. *Front Microbiol* **7:** 1–15.

Ryan, R.P., Vorhölter, F.J., Potnis, N., Jones, J.B., Van Sluys, M.A., Bogdanove, A.J., and Dow, J.M. (2011) Pathogenomics of Xanthomonas: understanding bacterium-plant interactions. *Nat Rev Microbiol* **9:** 344–355.

Santos, T.M.A., and Bicalho, R.C. (2011) Complete genome sequence of vB_EcoM_ECO1230-10: a coliphage with therapeutic potential for bovine metritis. *Vet Microbiol* **148:** 267–275.

Savary, S., Willocquet, L., Pethybridge, S.J., Esker, P., McRoberts, N., and Nelson, A. (2019) The global burden of pathogens and pests on major food crops. *Nat Ecol Evol* **3:** 430–439. doi: 10.1038/s41559-018-0793-y.

Schindelin, J., Arganda-Carrera, I., Frise, E., Verena, K., Mark, L., Tobias, P., *et al*. (2009) Fiji - an Open platform for biological image analysis. *Nat Methods* **9:** 1–15.

Schneider, C.A., Rasband, W.S., and Eliceiri, K.W. (2012) NIH Image to ImageJ: 25 years of image analysis. *Nat Methods* **9:** 671–675.

Schoonejans, E., Expert, D., and Toussaint, A. (1987) Characterization and virulence properties of *Erwinia chrysanthemi* lipopolysaccharide-defective, phi EC2-resistant mutants. *J Bacteriol* **169:** 4011–4017.

Seemann, T. (2014) Prokka: Rapid prokaryotic genome annotation. *Bioinformatics* **30:** 2068–2069.

Seemann, T. (2017) Shovill: Faster SPAdes assembly of Illumina reads.

Singer, T., and Burke, E. (2003) High-throughput TAIL-PCR as a tool to identify DNA flanking insertions. In *Methods in Molecular Biology, vol. 236: Plant Functional Genomics: Methods and Protocols*. Grotewold, E. (ed). Totowa, NJ: Humana Press, pp. 241–271.

States, D.J., and Gish, W. (1994) Combined use of sequence similarity and codon bias for coding region identification. *J Comput Biol* **1:** 39–50.

Steffens, T., Vorhölter, F.J., Giampà, M., Hublik, G., Pühler, A., and Niehaus, K. (2016) The influence of a modified lipopolysaccharide O-antigen on the biosynthesis of xanthan in *Xanthomonas campestris* pv. *campestris* B100. *BMC Microbiol* **16:** 1–14.

Sullivan, M.J., Petty, N.K., and Beatson, S.A. (2011) Easyfig: a genome comparison visualizer. *Bioinformatics* **27:** 1009–1010.

Sumrall, E.T., Shen, Y., Keller, A.P., Rismondo, J., Pavlou, M., Eugster, M.R., *et al*. (2019) Phage resistance at the cost of virulence: listeria monocytogenes serovar 4b requires galactosylated teichoic acids for InlB-mediated invasion. *PLOS Pathog* **15:** 1–29.

Svircev, A., Roach, D., and Castle, A. (2018) Framing the future with bacteriophages in agriculture. *Viruses* **10:** 1–13.

Vicente, J.G., Conway, J., Roberts, S.J., and Taylor, J.D. (2001) Identification and origin of *Xanthomonas campestris* pv. *campestris* Races and related pathovars. *Phytopathology* **91:** 492–499.

Vicente, J.G., and Holub, E.B. (2013) *Xanthomonas campestris* pv. *campestris* (cause of black rot of crucifers) in the genomic era is still a worldwide threat to brassica crops. *Mol Plant Pathol* **14:** 2–18.

Vorhölter, F.J., Niehaus, K., and Pühler, A. (2001) Lipopolysaccharide biosynthesis in *Xanthomonas campestris* pv. *campestris*: a cluster of 15 genes is involved in the biosynthesis of the LPS O-antigen and the LPS core. *Mol Genet Genomics* **266:** 79–95.

Wagemans, J., Blasdel, B.G., Van den Bossche, A., Uytterhoeven, B., De Smet, J., Paeshuyse, J., *et al*. (2014) Functional elucidation of antibacterial phage ORFans targeting *Pseudomonas aeruginosa*. *Cell Microbiol* **16:** 1822–1835.

Wagemans, J., Tsonos, J., Holtappels, D., Fortuna, K., Hernalsteens, J.-P., De Greve, H., *et al*. (2020) Structural analysis of jumbo coliphage phAPEC6. *Int J Mol Sci* **21:** 1–13.

Wanke, A., Malisic, M., Wawra, S., and Zuccaro, A. (2021) Unraveling the sugar code: the role of microbial extracellular glycans in plant–microbe interactions. *J Exp Bot* **72:** 15–35.

Wattam, A.R., Davis, J.J., Assaf, R., Boisvert, S., Brettin, T., Bun, C., *et al*. (2017) Improvements to PATRIC, the all-bacterial bioinformatics database and analysis resource center. *Nucleic Acids Res* **45:** D535–D542.

Wellington, E.M.H., Boxall, A.B.A., Cross, P., Feil, E.J., Gaze, W.H., Hawkey, P.M., *et al*. (2013) The role of the natural environment in the emergence of antibiotic resistance in Gram-negative bacteria. *Lancet Infect Dis* **13:** 155–165.

Wick, R.R., Judd, L.M., Gorrie, C.L., and Holt, K.E. (2017a) Completing bacterial genome assemblies with multiplex MinION sequencing. *Microb Genomics* **3:** 1–7.

Wick, R.R., Judd, L.M., Gorrie, C.L., and Holt, K.E. (2017b) Unicycler: resolving bacterial genome assemblies from short and long sequencing reads. *PLOS Comput Biol* **13:** 1–22.

Wick, R.R., Schultz, M.B., Zobel, J., and Holt, K.E. (2015) Bandage: interactive visualization of de novo genome assemblies. *Bioinformatics* **31:** 3350–3352.
Williams, P.H. (1980) Black rot: a continuing. *Plant Dis* **64:** 736.

Supporting information

Additional supporting information may be found online in the Supporting Information section at the end of the article.

Fig. S1. Basic phage characteristics of FoX2 and FoX6. (A) Infection curve of FoX2 on Xcc strain GBBC 1419 with the optical density (OD 600nm) in function of time in minutes. Error bars depict the standard deviation at a specific time point. (B) Infection curves of FoX6 on Xcc strain GBBC 1412 with the optical density (OD 600 nm) in function of time in minutes. Error bars depict the standard deviation at a specific time point. (C) Adsorption curves of FoX2 on GBBC 141 and FoX6 on GBBC 1412 as the percentage of non-adsorbed phages (P/P0) in function of time. Error bars indicate the standard deviation at a specific time point.

Fig. S2. Virulence assay of a subset of phage resistant knock-out mutants compared to wild type GBBC 1419 by assessing the percentage of symptomatic leaf tissue ($n = 15$). Mutants GBBC 1419a, GBBC 1419b and GBBC 1419d do not significantly differ from the wild type, although there is an effect on the virulence of GBBC 1419d. Mutant GBBC 1419c is less virulent compared to the wildtype GBBC 1419 (P-value = 0.0001 – non-parametric Dunnett's test; indicated with three asterisks). This result indicates a connection between virulence of GBBC 1419 and the epimerase/dehydratase protein.

Fig. S3. Multilocus sequence typing (dnaK, fyuA, gyrB and rpoD) of Xcc strains based on Cruz *et al.*, 2018. Strains isolated in this project are distributed among all clusters as previously described.

Fig. S4. (A) Log reduction of the bacterial concentration (CFU g^{-1}) 18 h after steeping artificially infested seeds with either FoX2 or FoX6. The reductions are calculated by subtracting the concentration of bacteria recovered after phage treatment (10^9 PFU added to the steeping water) from the concentration of bacteria recovered from the non-treated seeds (phage-less water). The effect of the same phage load was evaluated on different degrees of bacterial infestation of the seeds, 10^8 – 10^6 and 10^4 CFU g^{-1}, resulting in a phage MOI of 1, 100 and 10 000. It appears that the effect of the phages reduces with reducing numbers of target bacteria that are present on the artificial infected seeds. Error bars depict the standard deviation. (B) Log reduction of the bacterial concentration (CFU g^{-1}) 18 h after steeping with either FoX2 or FoX6 (10^9 PFU) on naturally contaminated seed. There was in both cases approximately a log 0.8 reduction (10^4 CFU g^{-1}) compared to the non-treated control (10^5 CFU g^{-1}). Error bars depict the standard deviation of three biological repeats.

Fig. S5. (A) Infection assay of FoX2 and FoX6 (MOI 1) on stationary cultures of GBBC 1419 and GBBC 1412, respectively, expressed as PFU ml^{-1} in function of time (in hours). Following the phage concentration over time shows that there is a minor phage production in case of FoX2 and FoX6, yet there is no net amplification of the phages compared to the initial phage concentration. Error bars depict the standard deviation. (B) Adsorption assay of FoX2 and FoX6 (MOI 1) on stationary cultures of GBBC 1419 and GBBC 1412, respectively. Here, the concentration of non-adsorbed phages is divided by the initial concentration of phage and plotted in function of time in hours. This assay shows that both phages are able to adsorb to their host, but that the production of phage progeny remains limited. Error bars depict the standard deviation.

Fig. S6. Seedlings developed from artificially infected seed (Xcc GBBC 1419 10^6 CFU g^{-1}) treated with 10^8 PFU ml^{-1} FoX2 14 days after sowing.

Fig. S7. Phage titer of FoX2 and FoX6 as isolated from the seedlings (PFU/seedling) when a concentration gradient of phage is given as a phytodrip treatment. A gradient of 10^6 – 10^7 – 10^8 – 10^9 – 10^{10} PFU ml^{-1} was added to cauliflower seeds. No phages could be recovered when 10^6 and 10^7 PFU ml^{-1} were given to the seeds. When the seeds received phytodrip of 10^8 – 10^9 and 10^{10} PFU ml^{-1}, phages were recovered at a concentration of 10^2 – 10^3 and 10^4 PFU/seedling (a log6 reduction of the initial dose) 14 days after treatment. As such, the concentration in the seedlings is dose dependent and the minimal concentration that needs to be administered is 10^8 PFU ml^{-1}.

Fig. S8. Prevention of symptom development (10 days p.i.) by irrigating phages (FoX6) to young cabbages ($n = 75$ per object) over a time span of six weeks as a percentage of infected tissue. Young cauliflower leaves were infected with GBBC 1412 by cutting the tips with scissors dipped in bacterial solution. No significant differences were observed in the percentage of symptomatic leaf tissue compared to the non-treated plants(mean 2% and median 1.4% symptomatic leaf tissue) and either of the phage treatments (108 PFU ml^{-1} mean 1.1%, median 0.95%, P-value of 0.1085- 109 PFU ml^{-1} mean 1.45% and median 0.83% of symptomatic leaf tissue, P-value of 0.18990). Blue areas represent the confidence interval and the blue line shows the median.

Fig. S9. Phage concentration at the leaf surface of cabbage leaflings in greenhouse conditions. A concentration of 10^9 PFU ml^{-1} was sprayed over the seedlings. After one and 24 h, three leaves were collected randomly and washed with PBS Tween 20 (0.1%) to elute the phages from the leaf surface. One hour after treatment, a concentration of 10^8 – 10^9 PFU ml can be recovered from the leaf surface. After 24h, this concentration dropped to approximately 10^7 PFU ml^{-1}. Error bars depict the standard deviation.

Fig. S10. The effects of 2 mM of $CaCl_2$ on the infection efficiency of Xcc on cauliflower (GBBC 1412 and GBBC 1419 – 10^6 CFU ml^{-1} – n = 30 plants). (A) The percentage of infected leaves and (B) The number of infection sites per infected leaf. In both cases, no difference is observed when $CaCl_2$ is added to the bacterial suspension (P-value > 0.05 – Wilcoxon/Kruskal–Wallis test).

Table S1. Gel-free mass spectrometry data from the capsid of phage FoX3. The structural proteins of one of the FoX1-like phages, FoX3, were identified experimentally using a gel-free mass spectrometry analysis of the phage capsids. As such, the hypothetical protein gp09 was established as

part of the structural locus of FoX3, as was the hypothetical protein gp19. Two proteins, gp33 (ssDNA binding protein) and gp38 (exodeoxyribonulcease VIII), also appear to be capsid-associated. Gene products gp51, gp76 and gp77 are also part of the viral capsid, but no potential function could be linked to these proteins based on homology to other proteins in the database at this time.

Table S2. Gel-free mass spectrometry analysis of the capsid of FoX6. Different conserved hypothetical proteins are presumably structural proteins as they are encoded within the same genomic region and were found to be part of the virion of FoX6. Moreover, the encoding genes are located in the same region of the genome, strongly suggesting that they make up the virion of FoX6.

Table S3. Host range of FoX1-7 on the Xcc collection as established in this research. For every strain the acquisition number, bacterial species, plant origin, geographical location and year of isolation are given.

